Water-food nexus: modelling the interlinkages between food prices, deforestation, and the water balance in northern South America

Master Thesis

Ajar Sharma

October 2017

Department of Water Management, Delft University of Technology

Water - food nexus: modelling the inter-linkages between food prices, deforestation, and the water balance in northern South America

By

Ajar Sharma

in partial fulfilment of the requirements for the degree of

Master of Science
in Civil Engineering

at the Delft University of Technology,
to be defended publicly on 30th October, 2017

Supervisor and Chair:	Dr. Saket Pande	TU Delft
Thesis Committee:	Prof. dr. Stefan Uhlenbrook,	TU Delft / UNESCO WWAP
	Dr. Boris van Breukelen,	TU Delft
	Dr. Lan Wang Erlandsson	TU Delft / SRC

This thesis is confidential and cannot be made public until October 31, 2017.

Preface

Dear Reader,

This thesis marks the completion of my Masters in Water Management at the Faculty of Civil Engineering and Geosciences, Delft University of Technology. This research has been performed under the supervision of dr. Saket Pande and prof dr. Stefan Uhlenbrook with the guidance from dr. Angela Renata Cordeiro Ortigara and dr. Lan Wang Erlandsson.

I would like to convey my gratitude to the Water Management Department's initiative towards research excellence. Dr Saket Pande's presence at the inception meeting of the UN World Water Development Report 2018 produced by World Water Assessment Program (WWAP) in September 2017 and his passion towards socio hydrology, gave birth to this thesis. I am deeply indebted to prof. Stefan Uhlenbrook and dr. Angela Renata Cordeiro Ortigara, for giving me the freedom to explore the subject, and also for supporting and guiding me when needed. I am grateful to my supervisor dr. Saket Pande, who has helped me throughout my work, and have guided me whenever I was stuck and needed inspiration. I would also like to thank dr. Lan Wang Erlandsson, who although being in Stockholm and working on her doctorate, found time and patience to answer all my queries. My special thanks to Nadja I. den Besten and Pradeep Rathore, for motivating me.

I would like to thank my close friends here in Delft, Hemant, Swaraj, Dhruv, Sruthi, Ioana, and others from the student board and the Dispuut Watermangment, who have made my stay in Delft extraordinary. My utmost gratitude to my parents for believing in my dream and providing me with endless love and support, without which I would not have reached this far in my life. Special thanks to Apoorva and Preeti for their care and understanding.

Nearly two years ago, I started with my Masters in Water Management after working for three years as a civil engineer in India. I never imagined that my dream to understand this fascinating field of water would bring me here. It has inspired me to take on this challenge and equipped me with the tools to make a difference, albeit small, through this research and the projects to come.

Ajar Sharma
Delft,
The Netherlands

Summary

Forests can influence local and regional weather and climate by various mechanisms. The importance of forests as a key regulator of moisture circulation has been shown by many studies. The Amazon rainforest is the lifeline for the conservation of the biodiversity of the region. However, since the last three decades, the deforestation trend in the region has increased. The local governments have passed legislation against illegal deforestation, specifically, the local governments of Mato Grasso state of Brazil have been the most vocal against the deforestation practices in its central and southern states. With cropping and animal grazing being one of the biggest reasons towards the clearing of the rainforest, often in response to growing global food demand, this research focused on a study to understand how the regional water balance and agricultural (soybean) induced land cover change in the region are interlinked. Soybean cultivation in the region is used as a proxy for the food demand in the water-food nexus.

A distributed hydrological and land cover coupled model has been developed and is used to interpret the changes in the region. A study area in the northern half of South America has been chosen. The water balance is carried out monthly and over a 1-degree by 1-degree pixel resolution. The precipitation in the region is modeled as a piece-wise linear function of the atmospheric moisture. Evaporation is calculated as a function of the transpiration rate at zero precipitation and the part of precipitation which is intercepted. With the help of empirical relationships and related parameterization, the total evaporation is calculated for the region. The forcing in the land cover change model is the soybean prices and the maximum monthly precipitation. Apart from being a cash crop, soybean is selected as one of the forcings due to its immense global demand in response to global food demand, with South America being the second biggest exporter in the world, and Brazil contributing the majority.

There are two sets of results presented, one for a time period of ten years and another for a thirty-year time period. The change in the study region's land cover on 1-degree by 1-degree resolution is presented along with the fractional change in the land cover types within each pixel. A major focus is put on the fraction change of forest and agriculture. Three sub-regions are selected to depict the change in downwind precipitation due to changes in land cover in the upwind regions. The regions are selected on the wind flow path along Bolivia and southern Brazil. R1, R2, and R3 are the regions from upwind to downwind side. The change in forest fractions is presented with the subsequent change in evaporation and precipitation in these sub-regions and subsequent feedback on land cover change from agriculture to savannas (i.e. abandonment).

Within a period of 10 years, on an average, a 3.6 percent reduction in the forest areas per 12,000 km^2 is observed. Within the same time period, the average increase in the agriculture areas is around 10 percent per 12,000 km^2, the average increase in the agriculture areas is around 10 percent per 12,000 km^2. This percentage increases to 28 for a period of 30 years. Soybean cultivation renders the soil without nutrients after two cycles of use and hence, new land is required for cultivation causing the abandonment of the previous land. These land cover changes have an impact on the evaporation and the precipitation in the regions. By subtracting the precipitation data for the modelled land cover scenario from the precipitation data for a constant modelled land cover, a coupling effect is demonstrated. Similar approach is carried out for evaporation as well.

R3 and R2 have average annual precipitation of 450 mm per year and 700 mm per year, respectively. For a period of 10 year, the maximum reduction of precipitation in the R3 and R2 region are 14 mm per year and 9 mm per year, respectively. For a period of 30 year, the maximum reduction of precipitation in the R3 and R2 region are 35 mm per year and 26 mm per year, respectively. R3 and R2 have average annual evaporation of 400 mm per year and 450 mm per year, respectively. For a period of 10 year, the maximum reduction of evaporation in the R3 and

R2 region are 12 mm per year and 11 mm per year, respectively. For a period of 30 years, the maximum reduction of evaporation in the R3 and R2 region are 33 mm per year and 32 mm per year, respectively.

There is a significant decrease in precipitation in the downwind region due to a reduction in forest cover in the upwind region. This decrease is also due to the reduced atmospheric moisture flow from upwind regions. Although the forest cover change is forced to change everywhere, the changes in the regions (R2) at the cusp of rainforest and savannas is studied. Rainforest which is closer to the existing agriculture areas is more susceptible to be cleared for animal grazing. The reduction in forest cover causes the evaporation in the region to reduce and which causes a reduction in the rainfall in the downwind region. Also, a continuous reduction in the precipitation causes the soil moisture deficit to grow and further reduce the evaporation. That is why the regions (R3) with lower precipitation and evaporation have higher reduction values. Therefore, it is concluded that there is a definite feedback between the land cover change and the change in precipitation. Since Amazon is going to play an important role in feeding the world population in the coming decades, it is of paramount importance that the area is conserved and utilized sustainably.

Contents

List of Figures

List of Tables

1. Introduction

1.1 Background

The Amazon rainforest spans around 7,000,000 km2 and covers countries like Brazil, Colombia, Bolivia, Venezuela, Ecuador, Peru, Surinam, Guyana and French Guyana. It is one of the most biodiverse places in the world. They are an integral part of the biosphere of South America [Satyamurty *et al*, (2013)]. The Amazon river is the largest river by volume and hence has an immense capacity to sustain life in the continent. For this reason, scholars have dubbed the Amazonian rainforest as the future lifeline of the world. Due to increasing world population, and limited areas and resources to grow food, it is high time that probable solutions are thought of.

Alick Bartholomew explains in his book, Hidden Nature: The Startling Insights of Viktor Schauberger published in 2004, the tropical rainforests are the powerhouse for balancing climate extremes in the planet. He recorded the vision of Viktor Schauberger, in which he compared the rainforest with the 'cradle of water', in a way that the rainforest produces the most balanced fresh quality water. These observations were made around 80 years ago, and now with modern technology and data availability, the theory is being proved.

According to World Bank, (2013), the world population will reach 9 billion by 2050 and to meet the future food demand, agricultural productivity will have to increase by 50-70 %. Latin America holds 28% of the potential new arable land, and even though some sub-regions are water scarce, it still holds the largest renewable water resource share. Hence, it is of paramount importance that we implement as many measures as possible to conserve the area. The Southeast region of the continent was identified as one of the five global food producing regions by Bagley *et al.*, (2012) due to the presence of ITCZ (Inter-tropical convergence zone) moisture movement. Also, in this region close to 15 % of the rainforest has been converted to agriculture and the vegetation in the region is prone to tipping over towards savannas due to reducing water vapour flows [Oyama and Nobre, (2003)].

Irrigation activities and deforestation both are major driving factors in terms of changing the regional hydrological cycle. Deforestation in the Amazonian rainforest has been discussed at length by various authors and has been advertised by various agencies. There are many reasons to the deforestation in the area, but the one that this research will focus on is the impact of agriculture. The decrease in water vapour flow in a region due to deforestation is generally compensated by increase water vapour flow due to irrigation, however, Amazon region does not receive any compensation from the irrigation vapour flows Gordon *et al.*, (2005). In the last three centuries, an approximate reduction of 7 to 11 million km2 in the forest area has been attributed to the agricultural expansion and timber extraction Foley *et al.*, (2005). According to INPE, (no date) (Brazil's National Institute for Space Research), 15% of the Brazilian Amazon has been cleared for agricultural purposes since the 1960s. The deforestation rate went up to approximately 25, 000 km2/year in the 1990s [Achard *et al.*, (2002)].

Prior to 2000s, the geophysical impacts of the deforestation were studied using the Global Circulation Models (GCM) by replacing the forest cover with grasslands, however, in the late 2000s, due to the availability of finer resolution data the parameterization improved substantially. Moore *et al.*, (2007) included variability of landscape and variability in external climate forcing. da Silva, Werth and Avissar, (2008) used the Regional Atmospheric Modelling System (RAMS), which is a complex and limited area model but was configured to include the

South America. Lejeune *et al.*, (2015) carried out simulations for four scenarios, business as usual, low deforestation, high deforestation and complete deforestation. The study focused on the increase of temperature due to deforestation and the effects thereafter. Laurance *et al*, (2004) found a non-linear relationship between the impact of deforestation and climate change attributing to the increased atmospheric CO2 levels, whereas, Macedo *et al.*, (2012) attributed the opposing trend from 2006 to 2007 to conservation schemes of the government.

PRODES (*Programa Despoluição de Bacias Hidrográficas* or Basin Restoration Program) has helped the Brazilian government to keep a strict vigil on the deforestation in the Legal Amazon. PRODES is operated by the INPE in collaboration with the Ministry of the Environment (MMA) and the Brazilian Institute of Environment and Renewable Natural Resources (IBAMA). It was estimated that in 2010, the forested region in Brazil has reduced to 80% of its original area from 1960. Davidson *et al.*, (2012) argued that Amazon rainforest may be a potential tipping point element in the earth system. It was based on the El Nino/Southern Oscillation (ENSO) affecting the rainfall in the area and consequently causing the Amazon river to lose volume. The narration at the end of the paper suggested that the changes in climate caused by deforestation may exceed the natural variability of climate. And it may affect the biomass, greenhouse gas cycle, and cycle of nitrogen, carbon, and water. Legislative wise, the Brazilian Forest Code has been immensely instrumental in the conservation of the rainforest. Despite the recent successful attempts to weaken the code, it still has been able to prevent deforestation and force reforestation outside the protected zones [Coe *et al.*, (2013)].

Although the land use practices change over the world, the final outcome in almost all the cases is the acquisition of the natural resources to satisfy the immediate human needs. The Latin America is conducive to a higher percentage of the agricultural production because of the tropical climate. They have been primary producers and exporters of a wide range of crops. Figure 1 shows the average export trend between 2010 and 2012. In order to meet future food demands, it is expected that soybean prices would shoot up as much as 15 % of their current prices in the next thirty years, which is the maximum among the crops grown in Latin America and the Caribbean (LAC) [Flachsbarth *et al.*, (2015)]. And not necessarily soybean cultivation but other types of crops (sugarcane, coffee, etc.) which are grown in the area and are exported due to huge global demand. The main issue with soybean is that after a couple of years of its cultivation, the soil is rendered barren. Since soybean is a cash crop, the farmers predicting higher profits, convert the grazing lands into agriculture fields. And in turn, the rainforests are converted into grazing fields. Directly or indirectly, the cultivation is responsible for encroachment towards the rainforest.

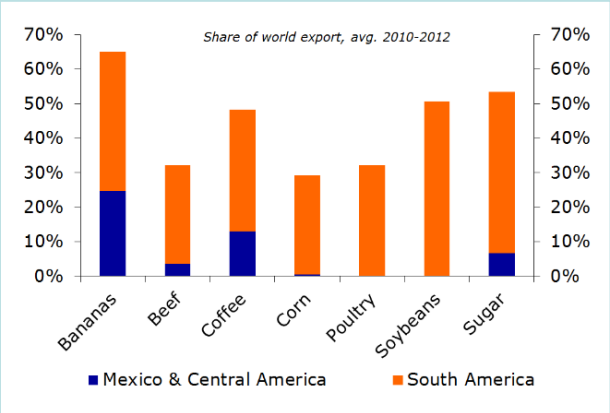

Figure 1 Share of world exports (average of 2010 - 2012). The graph depicts the major agricultural crops exported from Mexico and Central America, and South America as share of world exports. (Source: Source: UN Comtrade, FAO, Rabobank).

Bagley *et al.*, (2012) identified the evaporative source for soybean producing areas, between the cultivation months of November – April was largely terrestrial. Due to the presence of Andes in the west, the moisture source contributing towards soybean cultivation is from North and Northwest, with a majority fraction of evaporative source lying over the Brazilian Amazon.

The positive correlation between the deforestation in the region and the global soybean prices discovered in this research led to an intrigue towards how the relationship may change in the future. It is assumed that the decision taken by the farmers is based on the global prices of soybean and it takes a couple of years of a reverse trend for them to decide against growing soybean. It was observed in the Brazilian state of Mato Grasso during the period of 2005 – 2009, that although the global soybean prices increased, the deforestation values reduced. Macedo *et al.*, (2012) explained this by showing that the difference in agricultural production between 2001-2005 and 2006-2010. It was argued that during 2006-2010, 91% of the agricultural production took place on the previously cleared land. Another reason for the decrease in the soybean cultivation was an increase in the variable price (cost of seeds and fertilizers) of soybean as compared to what it was during 2001-2005. WWDR 2006, the second edition of World Water Assessment Programme's report suggested that even deforestation of 20% of surface area can potentially tip the Amazon basin to a point from where it cannot sustain itself, causing a complete collapse of the ecosystem with devastating impacts on the water security [UN-Water, (2006)].

It is clear that the soybean cultivation in the region for domestic use and for export is in contradiction with the climate protection objectives, which bat for a more sustainable use of the land. Due to an increase in monoculture system in the region due to soybean expansion, it competes with other crops for land and water requirements, which drives up the market prices. This may cause more farmers to cultivate crops like soybean and completely abandon other crop varieties, which is going to have a direct effect on the region's food security and climate resilience. In the region, the food crops are grown using rainfed conditions and therefore, loss of rainforest pose considerable food security risk because loss in atmospheric moisture due to deforestation is not compensated by irrigation, which is absent, induced additional evaporation [Bellfield and Sabogal, (2016)].

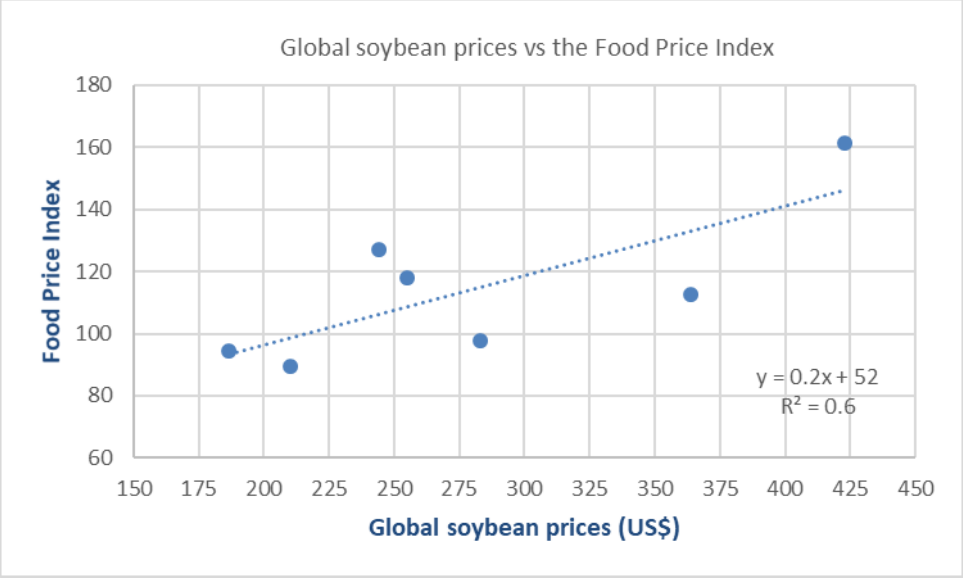

Figure 2 Correlation between the global soybean prices and the FAO food price index (FFPI). The graph justifies the use of global soybean prices as proxy for global food demand. (Source: World Bank)

Globally, soybean is cultivated to serve two major purposes; as livestock feed and for human consumption. In order to depict the nexus between food and water, interaction between global soybean prices and regional water balance is studied, where global soybean price is a proxy for

global food demand (see Figure 2). The latter is a fair assumption due to high correlation between global soybean prices and the global food price index (Figure 2). FAO food price index consists of the average of 5 commodity group price indices, namely, meat price index, dairy price index, cereals price index, vegetable oil price index, and sugar price index. The correlation between energy and soybean prices was not as significant as between soybean and food price index, and therefore was not considered. The biodiesel manufactured from the soybean oil is a high utility commodity, however, biodiesel generated from sugarcane performs economically better.

Moisture recycling and biotic pump theory contribute significantly towards the understanding of the effects of a reduction in forest cover on regional water balance. Moisture recycling is defined as the process in which a portion of the precipitated water that is evaporated from a region contributes to the precipitation of that region. Biotic pumping is a general case of moisture recycling which includes the change in land cover type and focuses on the importance of the presence of forest cover near the coastline. The moisture recycling studies have been carried out for many years now, with one of the initial studies done by a Russian climatologist M. I. Budyko [Budyko, (1972)]. In general, thermodynamics plays the primary role in terms of circulation of moisture in the atmosphere, i.e., colder, denser air sinks and hotter, lighter air rises.

Van Der Ent *et al.*, (2010) has shown for the global scale the sources and the sinks of the moisture recycling networks. In South America, the recycling percentage for the precipitation is 39 percent, which means that a greater percentage of the precipitation falling in the continent comes from the water evaporated in the same continent. Researchers like Eltahir and Bras, (1994) and Lettau, Lettau and Molion, (1979) have focused only on the river basins while studying moisture recycling.

Makarieva et al. (2013) focused on the major river basins of the world. They have shown that the precipitation values decrease as we move further inside of the continent and argue that if there are forests close to the coastline, the precipitation values would sustain even as far as 3000 km inside the coast. Makarieva and Gorshkov, (2006) found that the oceans are strong evaporators, the corresponding atmospheric moisture is then 'sucked' inland by the presence of forests along the coastline. Similar research done by Bunyard *et al.*, (2014) at the *La Selva* station in the Amazon forests claim a reduction of over 90% in precipitation as a consequence of deforestation and, therefore, desertification of the central part or west of the Amazon.

Makarieva, Gorshkov and Li, (2013) found that the biotic pump phenomenon in the Amazon rainforest reveals that the evaporation-condensation mechanism is the primary and a very powerful driver of the circulation of moisture in the area and thermodynamics is a mere secondary driver. The Brazilian portion of Amazon had up to 47.34% of its area affected by clear-cutting and degradation, what may be affecting the flow of atmospheric rivers that normally supply water not only for Amazon region but also for other areas in South America, including southeastern Brazil Dobrovolski and Rattis, (2015). Therefore, the biotic pump theory focuses on the vegetation and the importance of forest cover to show the impact of deforestation.

The United Nations (UN) first with the millennium development goals and then with the sustainable development goals have always been proactive in developing tools to quantify the actions required by the countries to work towards common goals. The Sustainable development goals were agreed on by the Member States of the UN in 2015 to achieve an ambitious set of targets by 2030. Sustainable use of the land surface and water resources is one of the goals. UN World Water Assessment Programme (WWAP) releases an annual report on a related topic which is aimed at providing comprehensive data regarding the theme and provide a synopsis of all that is going on in that field and next year, in 2018, the theme is "Nature-based Solutions for Water".

The SDG number 15 called as Life on Land, is defined as "protect, restore and promote sustainable use of terrestrial ecosystems, sustainably manage forests, combat desertification and halt and reverse land degradation and halt biodiversity loss" UNDP, (2015). As mentioned in the official website of the SDG, it is mentioned that the progress in preserving the ecosystems is not equal all around the world. It is asserted that from 2010 – 2015, the deforestation rates have reduced. However, the first major in-depth review of this goal is due in 2018. The session in 2018 is termed as "Transformation towards sustainable and resilient societies", and hence could be interesting to see how this transformation can be carried out by using nature-based solutions.

Food security and water availability are intricately linked to each other. Their proper management is required for sustainable development, which is impossible without understanding such interlinkages. At the river basin level, the interlinkage is strong as the demand of water between the upstream and downstream areas can increase the trade-offs in the cost of agriculture production Leck *et al.*, (2015). Drawing parallels between the food security and water availability, with the soybean production affecting the water balance of the region, this research tries to answer the interdependencies between them.

1.2 Research Question

The objective of this research is to understand and interpret the spatial and temporal interlinkages between the soybean prices, deforestation, and the regional water balance in northern South America. The objective is divided into the following research questions:

1. Based on current trends, to what extent may soybean cultivation cause further deforestation in the Amazon?
2. How do forest clearing and the abandonment that follows, affect the rainfall and evaporation patterns in the region?

1.3 Structure of this document

Chapter 2 (Data and Study Area) introduces the study area and the data used for creating the climate model in detail. It explains why the particular stretch of the area was selected. It also focuses on the various databases used. It focuses on why certain parameters were selected and how the data downloaded was converted to usable units.

Chapter 3 (Methodology) includes the methodology of the thesis and why a certain database was required. It also focuses on the underlying physical phenomenon that governs regional hydrology. The chapter also includes the coupling procedure and the validation procedure of the model. The connection between this coupling and how the model limitations affect them is also explained in detail.

Chapter 4 (Results and Discussion) addresses the research questions mentioned earlier in this chapter. This chapter provides the results of the procedure described in chapter 3 and then explains logically the validity of the results. It also explains the possible shortcomings of the coupled model

Chapter 5 (Conclusions and Recommendations) answers the research questions and provides most import findings from this thesis and possible recommendations.

2. Study Area & Data

2.1 Introduction

In this chapter, the study area for the research and the data used is discussed in detail. The study area is discussed first followed by the climate, topography, demography, and land use. The section includes the sources of suitable data and why a certain type of data was suitable for the chosen study area. The section also discusses the retrieval methods and the necessary corrections carried out for the data.

2.2 Study Area

The study area is situated in the northern part of South America which includes Brazil, Peru, Colombia, Venezuela, French Guyana, Suriname, Guyana, Ecuador, Bolivia and parts of Chile, Paraguay, and Argentina.

The study location is a 4, 140, 004 km by 5, 482, 708 km area in the northern part of South America shown in the figure below. The study area has the coordinates,
N 11.39, W -81.83, S -25.60, and E -32.83.

Figure 3 Study area showing the major countries and the major states.
(Source: Snipped off Google Maps on 19.09.2017)

It was initially thought of working on a country level, however, it was much more useful to not consider the political boundaries. The only constraints imposed were the geographical boundaries.

2.2.1 Climate

The climate pattern of South America can be divided into seven types; however, the majority of the study region is tropical. It is humid tropical and tropical savanna in the north and becomes dry at the bottom west corner, which is the tip of Atacama Desert (one of the driest places in the world). Venezuela and southern parts of Brazil have high temperatures throughout the year and receive rainfall in the summer only. Argentina, Uruguay, and Paraguay experience hot summers and cold winters with above average rainfall. Southern parts of Brazil, including the cities like Sao Paolo and Rio experiences warm to high temperatures with rainfall in autumn and winter months. And the majority of Brazil, Guyana, French Guyana, Suriname, Colombia experiences high temperatures and very high rainfall. The average rainfall in the Amazon basin is around 2000 mm per year. The main factor influencing the climate is the presence of pressure gradient zones over the Atlantic Ocean which determines the movement of the moisture bearing wind and the Intertropical Convergent Zone (ITCZ). Also, the Andes acts as the orographic barriers and cast a major rain shadow in the southern part of the continent and is one of the most important

boundary conditions in our model. The ITCZ follows the annual migration of the sun and reaches its most northerly position during the southern hemisphere's winter, which causes drying up of the region Dorst and Knapp, (2017) .

The Hadley cell circulation explains the generation of trade winds. Cold, dense and dry air sinks over Sahara Desert of Africa which forms a high-pressure zone. The south-easterly trade winds move from the south-east direction towards the equator and the northeasterly trade winds move from the north-east direction towards the equator, to form a converging are known as the Intertropical Convergent Zone (ITCZ). Depending upon the time of the year this zone shifts towards north and south of the equator. These trade winds bring heavy rainfall to the east coast of Brazil, throughout the year, however, on the west coast the trade winds blow westwards and are dry.

Table 2 and Table 3 represent the ten year monthly mean data of the countries lying in the study region. The countries lying in the vicinity of the Amazon basin receive heavy rainfall as compared to countries like Argentina, which are majority grassland covered.

Table 1 Ten year (2001 - 2010) monthly mean precipitation of the countries lying in the study region. It depicts the contrasting variation in the precipitation of countries lying in the study region. (Source: World Bank)

	Precipitation in mm per month								
	Argentina	**Brazil**	**Bolivia**	**Colombia**	**Ecuador**	**Guyana**	**Peru**	**Suriname**	**Venezuela**
January	66	236	196	109	184	173	188	198	46
February	64	232	182	110	209	141	205	181	39
March	74	243	150	213	272	132	216	195	55
April	47	188	76	252	276	234	142	266	134
May	35	141	48	365	221	378	121	369	242
June	26	80	20	328	138	346	90	284	324
July	24	64	24	307	209	309	82	244	327
August	24	53	24	249	107	197	64	158	272
September	31	71	38	228	83	108	75	66	190
October	52	122	85	280	134	94	129	61	167
November	54	156	99	255	168	97	153	76	137
December	66	216	156	184	144	225	176	188	95

Table 2 Ten year (2001 - 2010) monthly mean temperature of the countries lying in the study region. It depicts the variation in the temperature of countries lying in the study region. (Source: World Bank)

	Temperature in °C								
	Argentina	**Brazil**	**Bolivia**	**Colombia**	**Ecuador**	**Guyana**	**Peru**	**Suriname**	**Venezuela**
January	21.3	26.2	22.4	24.9	21.8	25.9	20.4	25.6	25.9
February	20.4	26.2	22.4	25.2	22.0	25.9	20.4	25.5	26.3
March	18.3	26.1	22.2	25.3	21.8	26.0	20.3	25.6	26.8
April	14.2	25.7	21.1	25.0	21.9	25.9	20.1	25.7	26.8
May	10.1	24.7	18.8	24.5	21.3	25.7	19.2	25.8	26.2
June	8.2	23.9	17.6	24.0	20.4	25.3	18.4	25.6	25.3
July	7.5	24.1	17.6	23.9	20.4	25.2	18.2	25.8	25.1
August	9.1	24.9	19.0	24.2	20.6	25.9	18.8	26.3	25.5
September	11.9	25.9	20.8	24.5	21.0	26.6	19.4	26.9	25.9
October	15.4	26.6	22.3	24.5	21.3	27.0	19.9	27.2	26.1
November	17.8	26.4	23.0	24.5	21.2	27.0	20.2	27.0	26.1
December	20.0	26.2	22.5	24.5	21.3	26.1	20.0	26.0	25.7

2.2.2 Topography and Land Use

South America is the fourth largest continent in the world and land of extremes. It has the largest river (Amazon), one of the driest places in the world and the Aconcagua mountain, which is the highest point in the western hemisphere. The topography of the continent can be divided into distinct land cover types, namely, rainforest, grassland, savanna, desert, deciduous forest, and alpine. The Amazon rainforest, which is the dominant land cover type in the continent WWF, (2016), is a complex and interdependent system of tropical rainforests and rivers which interact with the atmosphere.

World Bank, (2013) report on agricultural exports from the Latin America and Caribbean's (LAC), it was estimated that the 28 percent of the land suitable for sustainable expansion is in this region. Also, LAC has the highest renewable water endowment among the developing regions. The region also has an increasing share of the growing market and currently holds a much larger portion (13 percent) of the world trade in the agriculture sector Chaherli and Nash, (2013).

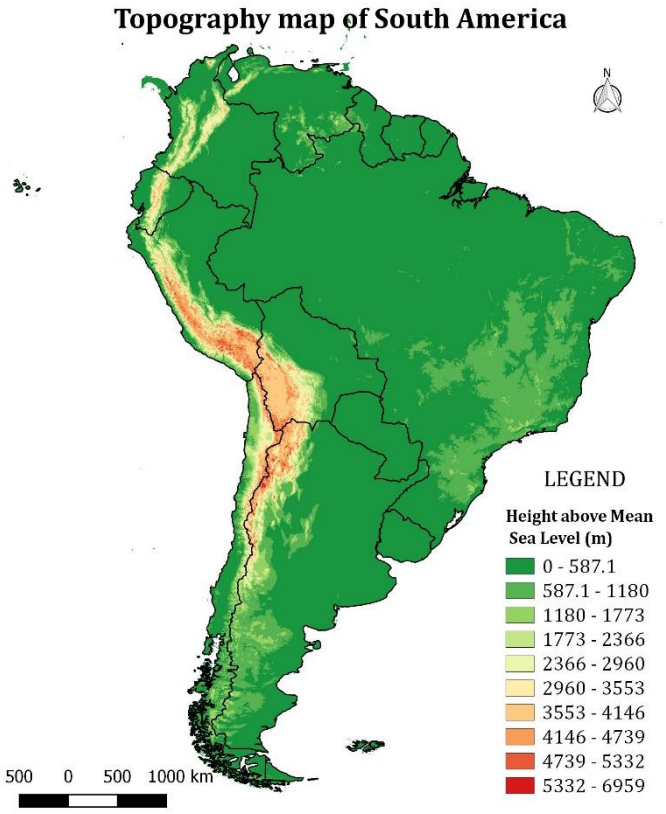

Figure 4 Topography map of South America depicting the different geographical areas with reference to the mean sea level(m). (Source: U.S. Geological Survey's Centre for Earth Resources Observation and Science)

Soybean production became one of the LAC's top ten export products in the first decade of this millennium. The current soybean boom is being driven by the need for food and the resulting financial gain. Due to the sheer growth of the human population, there is an unprecedented requirement for food. Turzi, (2012) found that in the same decade, the harvested area in Brazil increased by 53%, in Argentina by 63%, and in Paraguay by 94%. The investors in this region have dived into the agriculture market and converted the commodities into an asset class. This has given a huge impetus to the growing global agricultural export market in South America.

2.3 Data

There are two global geospatial datasets used in this research, i.e., ERA-Interim Berrisford *et al.*, (2009) and MODIS ORNL DAAC, (2017). The data acquiring technique for both the datasets is different. The ERA-Interim atmospheric model and reanalysis system uses European Centre for Medium-Range Weather Forecast's (ECMWF) Integrated Forecast System. The Moderate Resolution Imaging Spectroradiometer (MODIS) is part of TERRA and AQUA satellites. It plays an important role in validating, global interactive earth systems to predict global change effectively.

2.3.1 ERA-Interim

ERA-Interim project was initiated in the previous decade to assist in providing a bridge between ECMWF's previous reanalysis, ERA-40, and the upcoming reanalysis dataset at ECMWF. The actual objectives of this project were to critically improve on the ERA-40. Factors like the hydrological cycle, the quality of the stratospheric circulation, and the handling of biases and changes in the observing system have been significantly improved.

The instantaneous data like the vertical integral of water vapour and the zonal and meridional wind data were downloaded as the monthly mean of daily means. Boers *et al.*, (2017) found that the mean wind speeds between the pressure levels of 700 hPA and 900 hPa, remain similar to the wind speeds at 750 hPa. Therefore, the wind data is downloaded for the 750 hPa pressure level. The precipitation and evaporation data is downloaded for the 12 hourly monthly mean of the daily forecast accumulations Dee *et al.*, (2011). All the data, except the wind speeds, is downloaded on 1.0° latitude x 1.0° longitude grid resolution for a period of ten years from 2001 to 2010. The wind speed data is downloaded for the finest resolution available at the ERA-Interim, i.e., 0.125° latitude x 0.125° longitude.

The above datasets were downloaded for the N 11.39, W -81.83, S -25.60, and E -32.83 coordinates. The water balance calculations are done on monthly time data and necessary changes have been made accordingly to the downloaded data.

Table 3 ERA-Interim data used in the research. The table describes the main input variables used for this research along with their ERA-Interim code names and units.

Sr. No.	Data Name (ERA-Interim Code)	Units (daily means averaged over a month)
1	u wind at 750 hPa (u)	m/s
2	v wind at 750 hPa (v)	m/s
3	Vertically Integrated Water Vapour (p55.162)	Kg/m^2
4	Precipitation for the grid (tp)	m equivalent of water
5	Potential Evaporation for the grid (e)	m equivalent of water

2.3.2 MODIS

The MODIS land cover type dataset includes five classification schemes (IGBP global vegetation classification system, University of Maryland (UMD) scheme, MODIS – derived LAI/Fpar scheme, MODIS-derived Net Primary Production (NPP) scheme, and, Plant Functional type (PFT) scheme), which describe land cover properties derived from observations spanning a year's input of Terra- and Aqua-MODIS data. The final IGBP classification is carried out by using supervised decision-tree classification method.

The dataset used in the research is the MODIS (MCD12Q1) LAND COVER (Version 005). The lowest resolution the data available is 500m x 500m (0.004° latitude x 0.004° longitude) from 2001 to 2007. However, the data can be downloaded for any lower resolution as the data is interpolated based on majority percent area for the intended resolution. The data is in WGS84

projection (Coordinate Reference System) and available in all currently used data formats. The data is downloaded in the resolution of 1° latitude x 1° longitude for the years from 2001 to 2007. However, for this research's purpose, the data for 2001 was also downloaded for 0.01° latitude x 0.01° longitude, in order to calculate the individual fractions within the mask 1° layer.

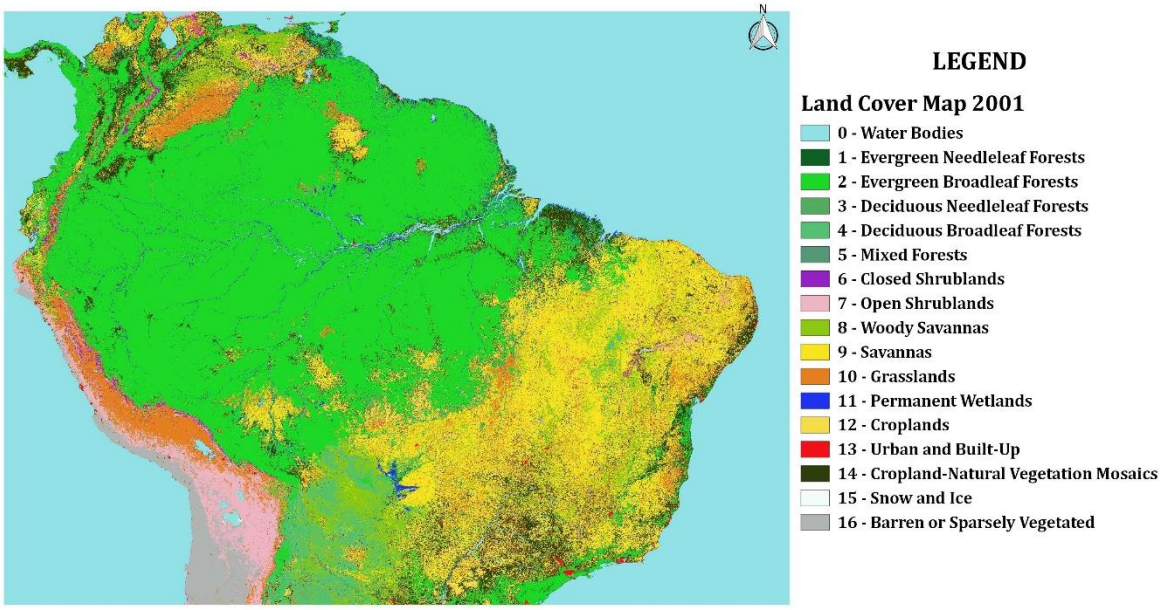

Figure 5 MODIS data for the year 2001. The figure depicts the land cover types in the highest resolution available as per IGBP classification

The above map is the highest resolution data available with the IGBP classification, however, for the purpose of this research the resolution and the land cover type is not required in such extensive detail. Therefore the 17 IGBP land cover types have been reduced to 4 basic ones, namely, Forest, Agriculture, Savannas, and, Water. The classification is modified to the following, with the country boundaries depicted in black.

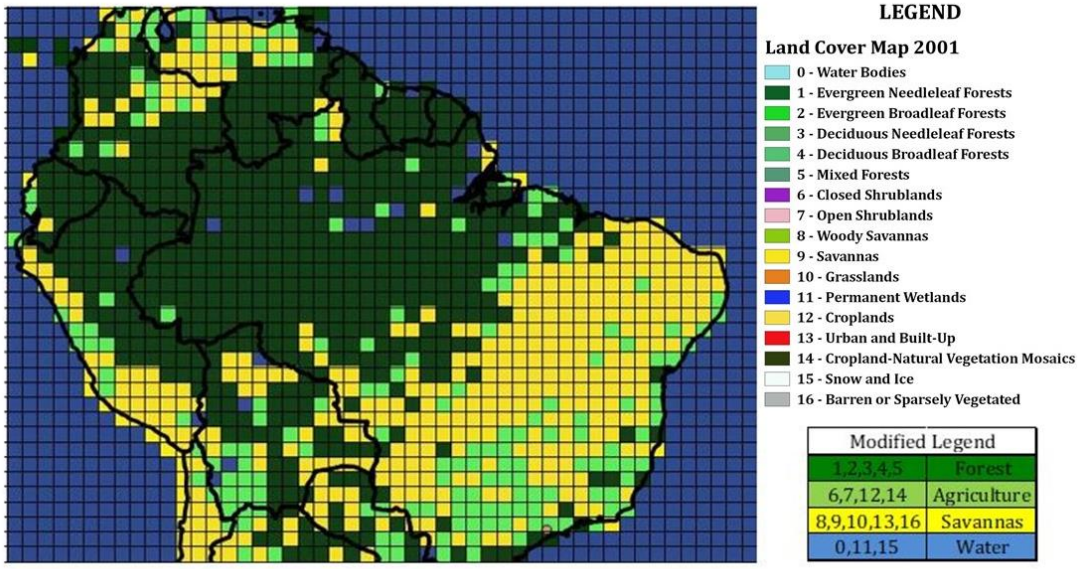

Figure 6 Modified land cover data from IGBP classification to four basic land cover types. (Shown above for 2001). The figure depicts the study area in 1-degree resolution with modified land cover types.

The above land cover types, when modified into four major land cover types, have the following partitions,

Table 4 The table shows the share of the different land cover types in the study region derived from MODIS data for the years from 2001 to 2007.

	Areas in km2			
	Forest	Agriculture	Savannas	Water
2001	6, 506, 520	1, 878, 891	4, 422,196	7, 425, 601
2002	6, 496, 561	1, 800, 342	4, 476, 128	7, 460, 175
2003	6, 485, 820	1, 759, 614	4, 538, 451	7, 449, 322
2004	6, 457, 959	1, 759, 054	4, 578, 285	7, 437, 909
2005	6, 425, 622	1, 855, 617	4, 497, 835	7, 454, 133
2006	6, 387, 691	1, 859, 645	4, 513, 836	7, 472, 148
2007	6, 387, 802	1, 860, 316	4, 512, 157	7, 472, 931

The next chapter explains how this data was modified and used for the purpose of this research.

3. Methodology

3.1 Introduction

This chapter explains the methodology of the research in detail. In order to understand the non-linear effects of land cover change upwind on the precipitation downwind, a non-linear model of moisture transportation in the study region is constructed. The simulations are carried out for ten years in order to capture the change in the land cover over these years, based on the forcing in this research, namely deforested land, soybean prices, and maximum precipitation. The simulations are also carried out on thirty years of data to understand the extent of change in that span. These simulations are also performed for the 'reference' condition where no land cover change is observed.

3.2 Water Balance

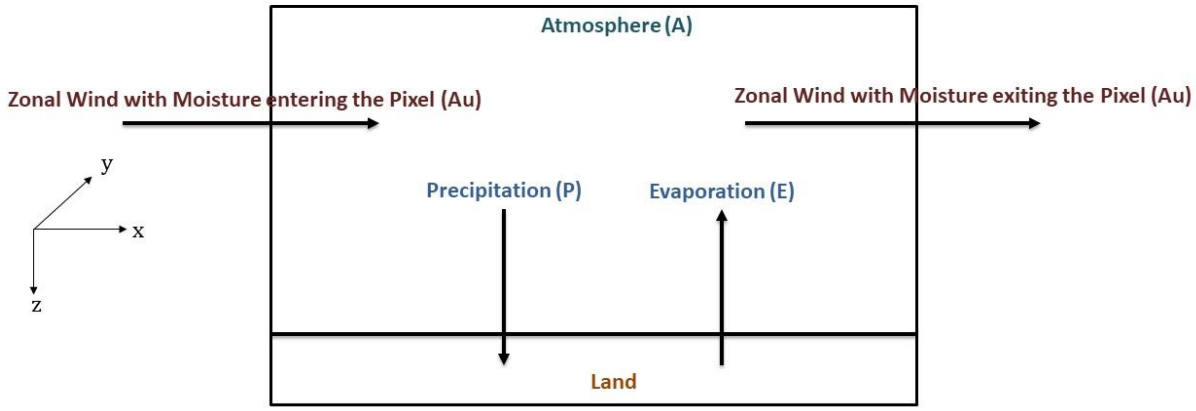

Figure 7 Illustration of atmospheric water balance. The figure shows the atmospheric moisture flowing in the zonal direction along with precipitation and evaporation. (Source: Eltahir & Bras, 1994)

The continuity equation dictates,

$$\frac{\partial A}{\partial t} = \frac{\partial (Au)}{\partial x} + \frac{\partial (Av)}{\partial y} + E - P \qquad [LT^{-1}] \qquad (1)$$

where, A is the vertically integrated atmospheric moisture storage (i.e., precipitable water), u and v are the wind components in x (zonal) and y (meridional) direction, E is the evaporation entering the atmosphere, and P is the precipitation removed from the atmosphere. The $\frac{\partial (Au)}{\partial x}$ is the horizontal moisture flux in the x-direction and $\frac{\partial (Av)}{\partial y}$ is the horizontal moisture flux in the y-direction. The direction of wind movement is due to the creation of low pressure zones due to the ITCZ. The air enters the region with velocities u, or v, normal to the boundary along with the moisture content A.

3.3 Regional water balance model

The data used in this model is from ERA-Interim as mentioned in the previous chapter. The events occurring outside the region considered may have an effect towards the final calculation of the moisture fluxes within the study area, which we ignore by repeating 10-year ERA-Interim atmospheric moisture at the boundaries. The model is run first for 10 years and then for 30 years to examine the land cover change based on the forcing.

The moisture enters the continent from the east along the intercontinental convergence zone over the Atlantic Ocean [Eltahir and Bras, (1994)]. The Andes in extreme west act as the barriers to the flow of moisture and due to orographic lifting as the moisture moves in the continent most of the moisture is precipitated in that region. The model assumes a strict division of the moisture entering the pixels. For simplicity, as is for many atmospheric models, the area is divided into square pixels and the data is assumed to be acting on the center of the pixel.

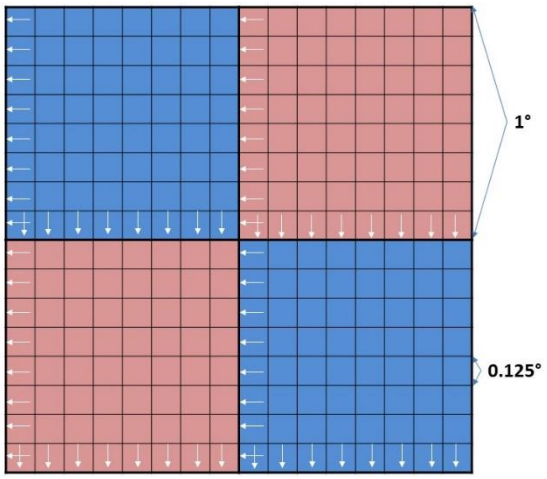

Figure 8 Illustration of wind speed data used with spatial distribution in 1° and in 0.125°. The lowest resolution data is used to minimise the error.

The moisture flow is calculated at the boundaries of the grid cell. The wind data at the resolution of 0.125° latitude by 0.125° longitude, is used to calculate the mean wind speeds at the boundaries. For every 1 ° resolution pixel, we have 8 x 8, 0.125° resolution pixels. For the zonal wind calculations, the boundary pixels on the left of the pixel are used and for the meridional wind calculations, the boundary pixels at the bottom are used. The schematic is shown on the left. The final velocity is taken as the mean of these eight-pixel data. The model uses a monthly mean wind speed over all the years, in order to control the variation and possible instability.

Implicit Euler scheme [Kavetski and Clark, (2010)] is used to discretize the differential equation, with the time step being one month and with 50 iterations over every month to get the most stable solution. If $\Delta x = \Delta y = Length\ of\ a\ pixel$, and $\Delta t = 1\ month$, then equation comes out to be as follows,

$$A_{xy,(t+\Delta t)} = A_{xy,t} - \left[\frac{u_{xy,t}\delta_x(A_{xy,t}) + A_{xy,t}\delta_x(u_{xy,t})}{\Delta x} + \frac{v_{xy,t}\delta_y(A_{xy,t}) + A_{xy,t}\delta_y(v_{xy,t})}{\Delta y}\right] * \Delta t + E_{xy,t}(P_{xy,t}) * \Delta t - P_{xy,t}(A_{xy,(t+\Delta t)}) * \Delta t \quad (2)$$

where $\delta_x(z_{xy,t})$ function defined as $z_{(x+\Delta x)y,t} - z_{xy,t}$. The divergence is taken in wind ($A_{xy,t}\delta_x(u_{xy,t})$) as well as the atmospheric water ($u_{xy,t}\delta_x(A_{xy,t})$). Similarly, for the meridional wind. Further, $E_{xy,t}(P_{xy,t})$ is the evaporation from the pixel modelled as a function of precipitation on the pixel and $P_{xy,t}(A_{xy,(t+\Delta t)})$ is the precipitation on the pixel modelled as a function of atmospheric moisture. These relationships are discussed later.

The wind flow patterns are shown in the figure below. It is interesting to take note that there is heavy convergence during the January (wet season) month from the North-East regions into the continent, however, in July (dry season) month, the wind pattern almost reverses. This reversal of winds brings in the moisture from the Caribbean into the Amazon, which causes shifting of monsoons from above and below the equator.

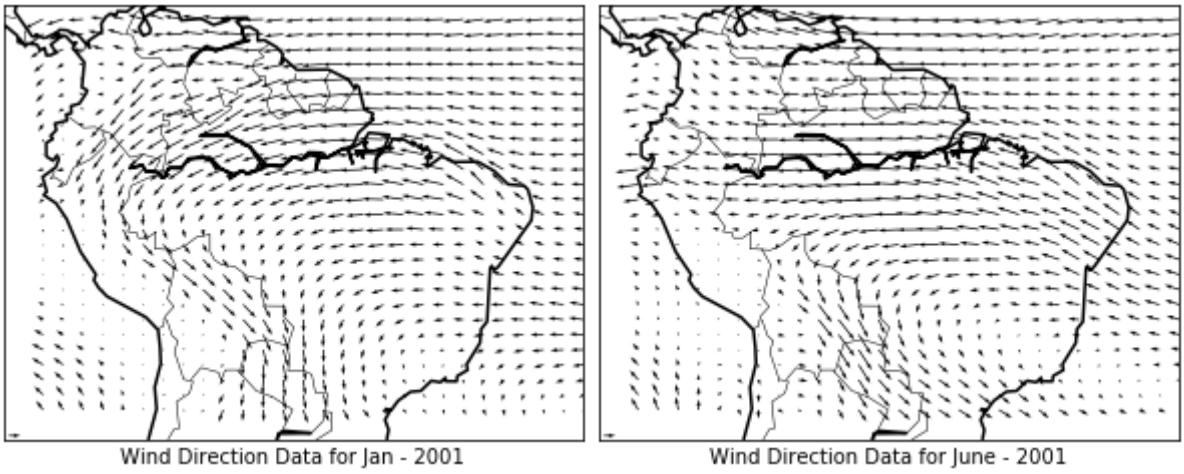

Figure 9 Wind flux of the study region for the months of January and June in 2001. The data depicted above is the daily average for the respective months in meters per second.

The precipitation is assumed to be a function of the atmospheric water vapour because logically, there should be a threshold value between the actual rainfall and the atmospheric water vapour [Boers *et al.*, (2017)]. There is always a certain amount of moisture in the atmosphere which does not contribute into the final rainfall [Savenije, (1996)]. It is observed that the increase in precipitation with the increase in atmospheric water vapour is not linear.

For higher water vapour values, the precipitation increases with a higher gradient. Therefore, instead of a linear relationship between the precipitation and the atmospheric water vapour, this research has established a piece-wise linear function between the two. To further reduce the linearization, the atmospheric water vapour and precipitation data were segregated based on the modified land cover data. Therefore, different relationships for the four different land cover types were established as shown in the figure above.

The minimum water vapour carrying capacity over the forested area is the highest, as compared to the other three land cover types. Scott, (2016) attributed this to the roughness of the surface of forests. The winds passing over a non-forested region will pass over it without any disturbance. The general form of the relationship between precipitation and atmospheric water vapour is assumed to be as follows,

$$P(A) = k + A * \alpha \quad (3)$$

where k and α are parameters that change with different ranges of A as shown in Figure 10.

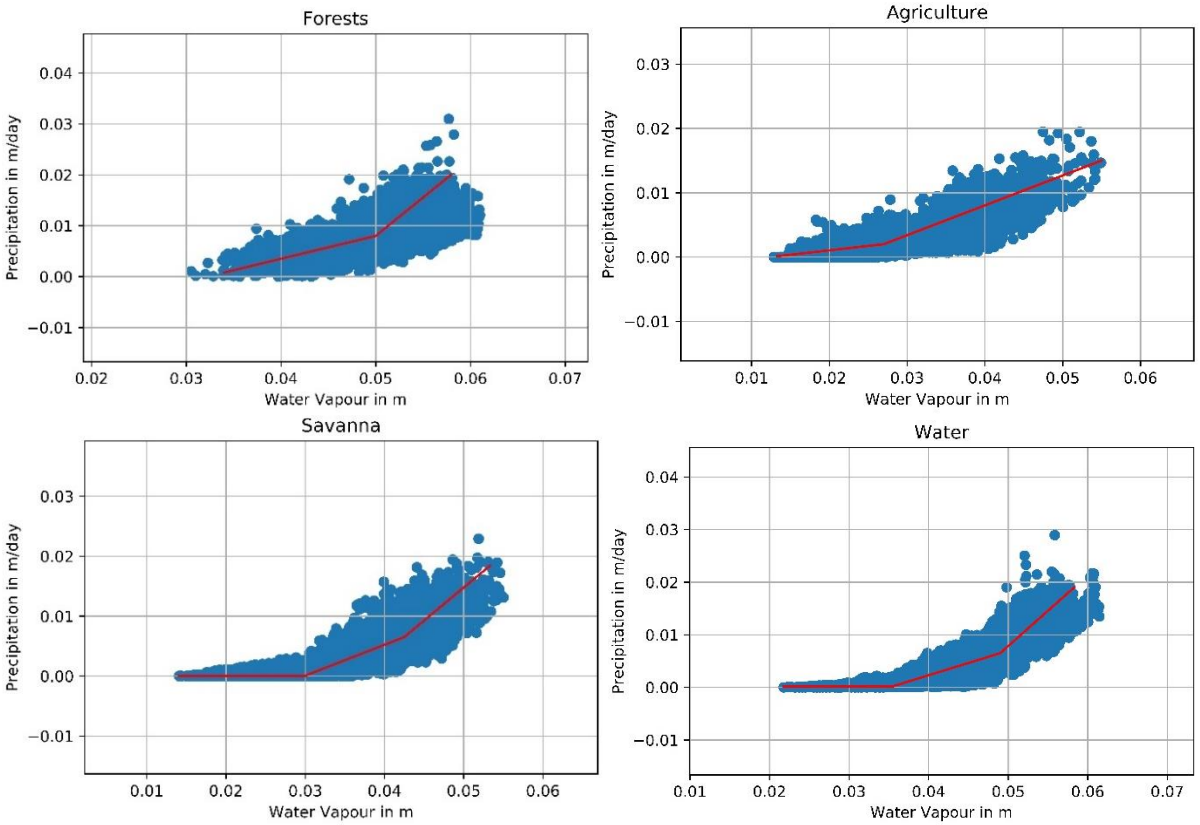

Figure 10 Scatter plot of precipitation P versus atmospheric water vapour A. Piecewise linear best fit is used to include the non-linearities in the data.

The land cover type fractions (forest, agriculture, savannas, and water) calculated from landcover map at 0.01° x 0.01°, for every 1° x 1° pixel, are calculated based on the available MODIS datasets for the base year 2001. The precipitation is calculated for every pixel using its respective relationship with the atmospheric water vapour and the respective land cover fractions. If P represents the precipitation in the 1° pixel and, P_f, P_a, P_s, P_w are landcover specific precipitation at 0.01° resolution, and f_f, a_f, s_f, w_f, are the forest fraction, agriculture fraction, savanna fraction, and water fraction, respectively, at 1° resolution calculated based on 0.01° data, then total precipitation in the pixel is given by

$$P(A) = P_f(A_f) * f_f + P_a(A_a) * a_f + P_s(A_s) * s_f + P_w(A_w) * w_f \quad (4)$$

Note that P_f, P_a, P_s, P_w are function of atmospheric moisture A at 1° resolution. Along with the atmospheric parameters, it is also important to ascertain the sub-surface processes and its parameters. In this research, we have used the concept of Maximum Climatological Water deficit (MCWD), which is the most negative value of the climatological water deficit Malhi *et al.*, (2009). It is determined for every pixel, based on the contemporary precipitation and evaporation values.

This approach is used by Zemp *et al.*, (2017) to create their cascading model framework for the Amazon rainforest. The equation used by them is modified as follows,

$$C(t) = C(t - \Delta t) + \big(P(t) - E(t)\big) * \Delta t \quad (5)$$

where t is the current time step, Δt is the previous time step, *P(t)* is the precipitation on the pixel at time t, and *E(t)* is the total evaporation from the pixel at time t and *C(t)* is the current water deficit. The current water deficit is added to the model in order to include a residence storage in the soil which is not affected by the runoff from the system [Malhi *et al.*, (2009)]. It is used to calculate A_m, which represents the transpiration rate when precipitation is zero. A_m is a carry-over factor that is related to the access of vegetation to subsurface water during seasonal drought. It depends upon the rooting depth and soil moisture [Zemp *et al.*, (2017)].

$$A_m(t) = \ -p_3 * C(t) + p_4 \quad (6)$$

$$E(t) = min(A_m(t) + \frac{P(t)}{p_1}(1 - \exp\left(-\frac{p_2}{P(t)}\right)),\ E_p(t)) \quad (7)$$

where, E_p is the potential evaporation and p_1, p_2, p_3 and p_4 are parameters dependent upon land surface properties (vegetation and soil) and daily rainfall characteristics Zemp *et al.*, (2017). These parameters were estimated for each vegetation state using iterative least-square based function in Matlab. p_1 and p_3 are dimensionless and p_2 and p_4 have the dimensions of flux (LT^{-1}). Evaporation equation is also modified to accommodate the land cover fractions. Similar to the precipitation equation above, if E represents the evaporation in the 1° pixel and, E_f, E_a, E_s, E_w are the evaporation components in the 0.01° for respective land cover types, and f_f, a_f, s_f, w_f, are the forest fraction, agriculture fraction, savanna fraction, and water fraction, that are calculated based on 0.01° data, respectively, then the equation 7 is modified as follows,

$$E_{f(t)} = A_m(t) + \frac{P_f(t)}{p_1}(1 - \exp\left(-\frac{p_2}{P_f(t)}\right)) \quad (8)$$

Similarly, for the other land cover types, the equation is changed and the minimum condition with the potential evaporation is not applied to this modified condition.

$$\mathrm{E}\ = E_f(P_f) * f_f\ +\ E_a(P_a) * a_f\ +\ E_s(P_s) * s_f\ +\ E_w(P_w) * w_f \quad (9)$$

For modeling purposes, the lower limit of precipitation is set as 10^{-5}, as the precipitation ends up in the denominator in the equation 8. In this research, due to the same study region, the parameters simulated by Zemp *et al.*, (2017) are used. The parameters are estimated for three vegetation states by them, namely, high tree cover, low tree cover, and, no tree cover. We have modeled forest using high tree cover parameters, agriculture with low tree cover parameters, and savannas with no tree cover parameters. For the water pixels, the potential evaporation is assumed to be equal to the actual evaporation. However, p_1 values were modified to calibrate to the requirements of the model.

Table 5 The parameters p_1, p_2, p_3, p_4 calculated on ERA-Interim data for the three separate land cover types. p_1 and p_3 are dimensionless whereas, p_2 and p_4 have the dimensions of flux[LT^{-1}] (Zemp et al., 2017)

	Forest	Agriculture	Savannas
p_1 [-]	1.44	2.01	1.78
p_2 [LT^{-1}]	5.48	6.44	3.45
p_3 [-]	-1.04	-0.25	-0.32
p_4 [LT^{-1}]	2.26	1.69	1.60

The water balance simulations are carried out at monthly time steps. The first 12 months of the run of the simulations are assumed to warm up period, therefore, the output for the last nine years is considered. In order to control the numerical instability, the atmospheric water vapour is designed as a double layered system, where the flow of atmospheric water takes place in the top layer and the precipitation and the evaporation interact with the bottom layer. There is a generous ceiling on the atmospheric water content carrying capacity over a pixel, which controls the instability, if any, in the system. Further an interpolation scheme is implemented to control numerical instability that smooths, via interpolation, atmospheric moisture field at each time step. In this research, out of a bivariate spline interpolation and a nearest neighbour interpolation schemes, the later one is chosen. Due to high variability in the grid data, the bivariate spline interpolates over the whole area results in over smoothening, which is undesirable. In case of nearest neighbour analysis, the closeness of interpolation can be defined. Out of the various grid options, the nearest neighbour interpolation in a 5x5 grid performed the best on our data sets, and hence, that is implemented in the model.

3.4 Land cover land use change model

The regional water balance model, which is a coupled atmospheric and soil moisture model as discussed above, is coupled with the land cover by the modeled precipitation, soybean prices, and the land cover fractions. In this research, we focus on the two land cover change signals, namely, conversion of forest to agriculture, and agriculture to savannas. The forcing factor in the conversion from forest to agriculture in the study region is taken as the global soybean prices. As explained in the introduction, statistically, there is a high correlation between the deforestation happening since 2001 and the soybean prices. Figure 11 depicts the relationship between the soybean prices and the deforestation for the study region.

The results of the linear regression between the deforestation data and the annual global soybean prices are statistically significance ($p < 0.05$). Therefore, for conversion from forest agriculture, the output coefficients of this regression are used in the transition matrix. Similarly, for the conversion from agriculture to savanna, the linear regression between the change in agricultural area over time and the maximum precipitation in a year show statistical significance. These two relations are used to quantify the change in the land cover over a year.

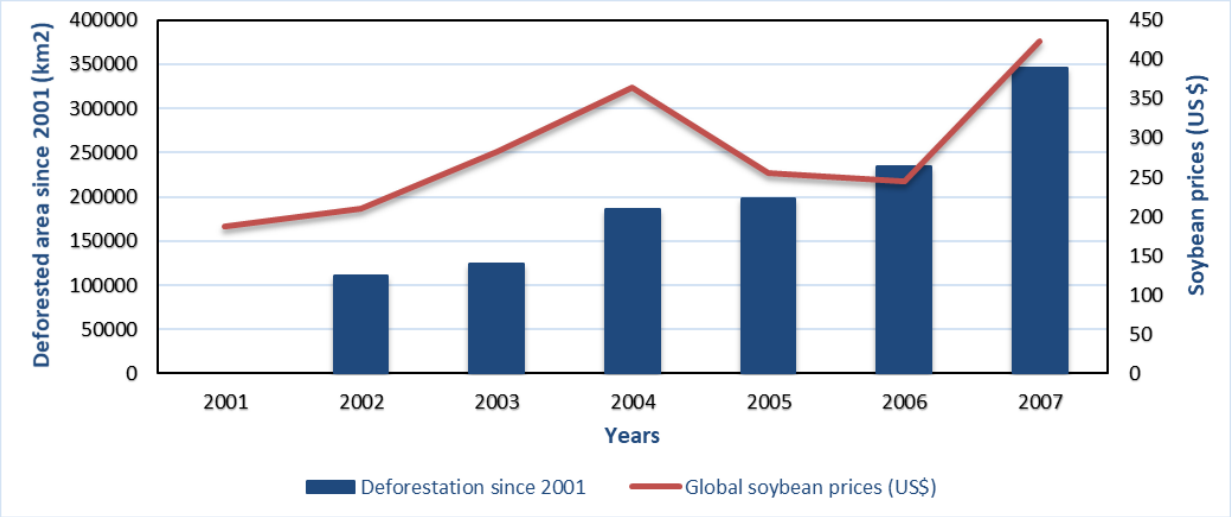

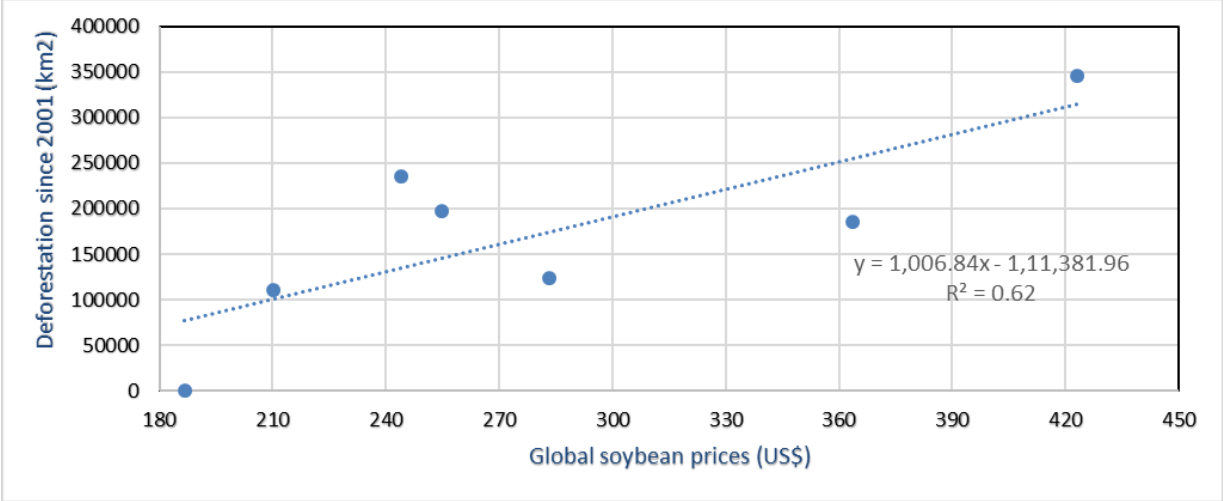

Figure 11 (Top)The figure shows the deforestation data since 2001 extracted from MODIS with the global soybean prices depicted on a secondary axis. (USDA),
(Bottom) This figure shows the high correlation between the deforestation since 2001 and the global soybean prices.

The model consists of two steps, first, the change is calculated and second, based on the change fractions of land cover for the next year are allocated. This research uses a simplified formulation of Conversion of Land Use and its Effects' (CLUE) concepts. The land use demand is not taken into consideration and the change is forced everywhere in the region and only the forward feedback is considered as shown in Figure 12.

Figure 12 Illustration of the modeled land cover change, where only forward feedbacks are assumed.

The transition matrix, T, is composed of empirical relationships, which outputs the change in a fraction within each pixel. If $\Delta\alpha_t$ is a land cover change vector $(\Delta f_f, \Delta a_f, \Delta s_f, \Delta w_f)$ then land cover change is modelled as,

$$\frac{\Delta\alpha_t}{\Delta t} = T * \alpha_t \quad (10)$$

Thus, total change in the fraction over a column should remain zero. There is no direct change happening in the fraction of savanna, therefore, that column is kept zero.

Table 6 The land use change/conversion matrix T depicting the notations used in the equations and their physical meaning.

	Forest	**Agriculture**	**Savannas**
Forest	-T21 Fraction which stays forest	0	0
Agriculture	T21 Fraction converting from forest to agriculture	– T32 Fractions converting from agriculture to savanna	0
Savannas	0	T32 Fractions staying savanna	0

T21 – This is the fraction of forest converted to agriculture, the forcing factors are the global soybean prices. The deforestation data from 2001 to 2007 is calculated based on MODIS data sets. Similar calculations are carried out to determine changes in agricultural and savanna areas. According to the transition matrix shown in Table 6, a negative change in forest area fraction is a positive change in agricultural area fraction.

Thus, T21 is $\frac{-\Delta f_f}{\Delta t}/f_f$, i.e. deforestation rate per unit forest fraction, which is expected to be a function of soybean prices as shown in Figure 11. In order to enforce a condition that no deforestation happen when soybean prices are 0, the fractional change in forest are regressed with soybean prices, keeping the intercept zero. Results are displayed are displayed in Table 7.

Table 7 Calculations for the transition matrix coefficients for T21 by using the fractional change in agricultural area

	Forest Area (km^2)	Agriculture Area (km^2)	Change in Agriculture area (km^2)	Fractional Change	Soybean Prices (US$) ($S_p$)
2001	6,506,520	1,878,890	0.00	0	186.65
2002	6,496,561	1,800,342	-78,548	$-1.2 * 10^{-2}$	210.22
2003	6,485,820	1,759,614	-40,729	$-0.62 * 10^{-2}$	283.21
2004	6,457,959	1,759,054	-560	$-0.008 * 10^{-2}$	363.55
2005	6,425,622	1,855,617	96,563	$1.50 * 10^{-2}$	254.74
2006	6,387,691	1,859,645	4,028	$0.06 * 10^{-2}$	244.00
2007	6,387,802	1,860,316	671	$0.01 * 10^{-2}$	423.08

T32 – This is the fraction converting from agriculture to savannas, i.e. abandonment, forced by changes in maximum precipitation in the year. The conversion from agriculture to savanna is calculated by dividing the change in the total savanna area with the actual agriculture area for that

year. Maximum precipitation is only calculated for the pixels which convert from agriculture to savanna between any two consecutive years from 2001 to 2007 (see Table 8). Finally, T31 value is obtained as a linear function of maximum precipitation of the corresponding year (see Table 9).

Table 8 Calculations for the transition matrix coefficients for T32 using the fractional change in the savanna area

	Agriculture Area (km^2)	Savanna Area (km^2)	Change in Savanna area (km^2)	Fractional Change	Maximum Precipitation (m per month) (P_{max})
2001	1,878,891	4,422,196	0	0	N/A
2002	1,800,342	4,476,128	53,932	$2.99 * 10^{-2}$	0.119
2003	1,759,614	4,538,451	62,324	$3.54 * 10^{-2}$	0.143
2004	1,759,054	4,578,285	39,834	$2.26 * 10^{-2}$	0.043
2005	1,855,617	4,497,835	-80,450	$- 4.33 * 10^{-2}$	0.129
2006	1,859,645	4,513,835	16,001	$0.86 * 10^{-2}$	0.158
2007	1,860,316	4,512,157	-1,679	$- 0.09 * 10^{-2}$	0.199

Table 9 Regression analysis output values for the T21 and T32 variables of the transition matrix T showing the parameter values, R-square values and the P-values.

Independent Variable	Parameter value	R-square	P-value
Soybean Prices for T21	$1.3 * 10^{-5}$	0.81	0.0149
Intercept for T32	0.026	0.23	0.5369
Maximum Precipitation for T32	- 0.128	0.23	0.6608

Therefore, the equations used in the model for further calculations are as follows:

$$T21 = 1.3 * 10^{-5} * S_p(t) \quad (11)$$

$$T32 = 0.026 - (0.128 * P_{max}(t)) \quad (12)$$

The fraction allocation procedure is described in the flowchart below. For model calculations, step 1 to 6 is repeated every year. The transition matrix receives the soybean data and the maximum precipitation for the year as input to the equations for T21 and T32. Based on the current area matrix and the transition matrix equations, the change in fractions is calculated. This change is then added to the existing fractions file to calculate the new fractions for the next year. This is the operationalization of equation 10, which is initialized with MODIS data area fractions for year 2001.

For visualization, based on the fractions data, the new land cover data at 1° is generated based on the maximum fractions condition, i.e., the land cover type with maximum fraction becomes the new land cover type for the pixel. The same procedure is carried out for 30-year simulations, with the exception of the input data. The atmospheric moisture for the boundaries, the potential evaporation, the wind speed data and the soybean prices data, are cycled for every ten years (i.e. 3 times, each repeating 10-year cycle). The 1° data calculation is for visualization purpose only, all the calculations within the model are carried out at 0.01° resolution.

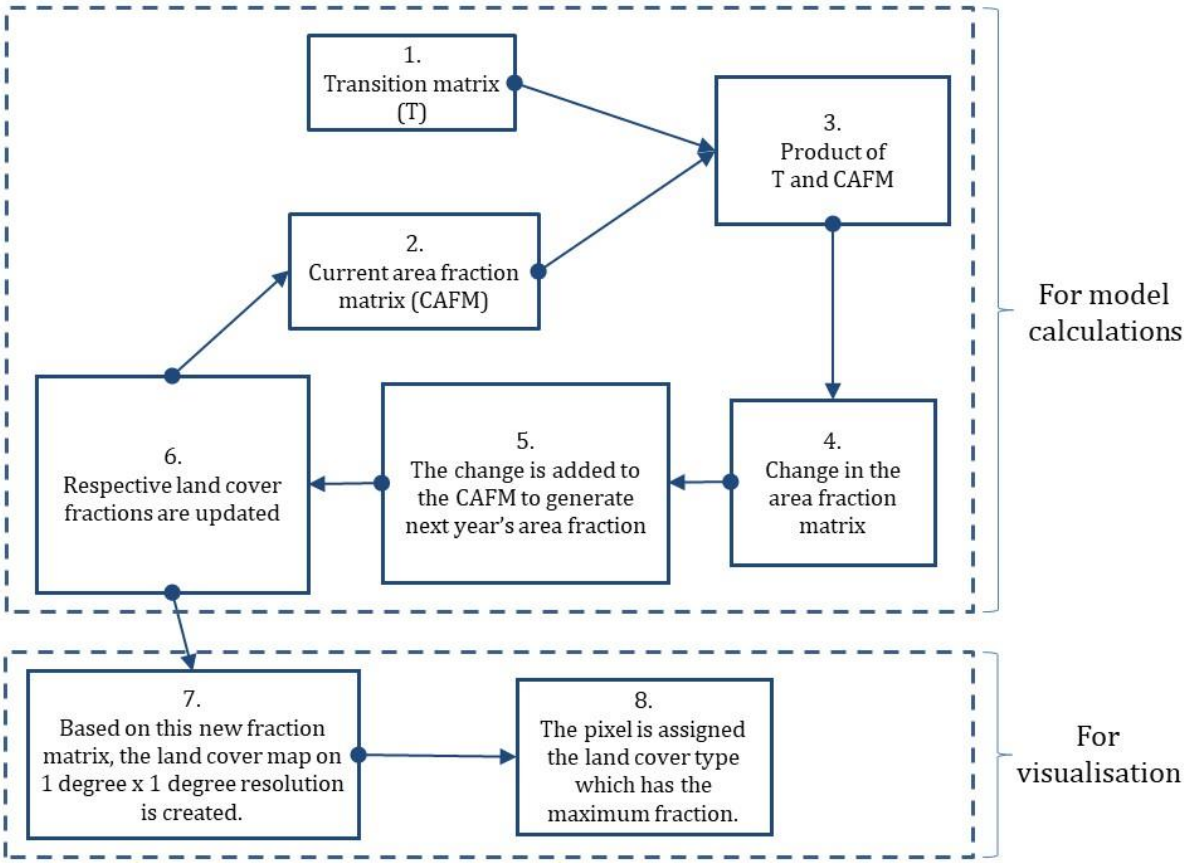

Figure 13 Flowchart depicting the fractions change and assignment for both model calculations and visualisation. Step 1 to 6 is used in the model calculations, whereas, step and step 8 are only used for visualising the land cover change after every year.

4. Results and Discussion

4.1 Introduction

The results for the 10-year simulations and 30-year simulations are presented together. First, the entire study area's land cover change is shown to identify the possible hotspots. Also, the fractional change in the agriculture and the forest are displayed. As the change is forced throughout the study area, also the remote Amazon locations, a set of three connected areas are selected. In order to show the biotic pumping effect, the areas were selected to be on the wind path. Proximity to the existing dwellings is also one of the criteria for selecting the areas.

4.2 Model Validation

The model is validated using the ERA-Interim reanalysis data. The two sets of plots for precipitation and evaporation are to show the validation for the model. Three regions (R1, R2 and R3; see Figure 14) are selected within the study region based on the wind maps. As wind is the carrier of moisture, the three regions are selected in such a way that they are in line with the moisture movement and have three distinct land cover type. The area of central Amazon is not considered due to the understanding that change is maximum in areas which are on the cusp of changing land covers between the rainforest and the agriculture. R1 is predominantly forest and part of the Amazon basin and therefore tropically wet. R2 is a mix of all the three land cover types and lies near the point of where the Amazon rainforest starts. R3 is majorly savanna and therefore has a tropically dry climate. Every region has 30 pixels each. The wind pattern depicted here is the daily average value of the month of January 2001.

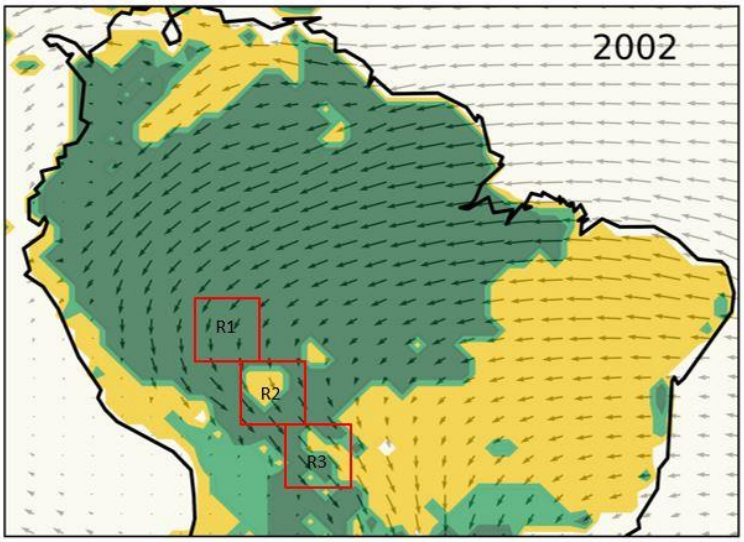

Figure 14 Figure shows the three regions used for validation. The map depicts the land cover pattern for 2002 with January's wind flow pattern.

Figure 15 presents the validation results for precipitation and evaporation with root mean square errors (RMSE) shown in the inset. The observed and modeled data often looks a little different to each other. The observed data uses a more comprehensive modeling approach, where model states are continuously updated by using the forecasted (within ERA-Interim) data twice a day. The model data underestimates the precipitation in the first region, which can be attributed to the fact that the ERA-Interim data is not a reliable gauge calibrated dataset and hence performs moderately well in forested regions. Boers *et al.*, (2017) found that the ERA-Interim reanalyses

data underestimates the precipitation in the western tropical South America. Betts, Köhler and Zhang, (2009) in a study to compare the ERA-Interim and ERA–40 datasets found that the former always overpredicts the precipitation in the Amazon river basin and the seasonal amplitudes are too small. However, in regions with relatively less dense forest, the observed and modeled datasets look analogous.

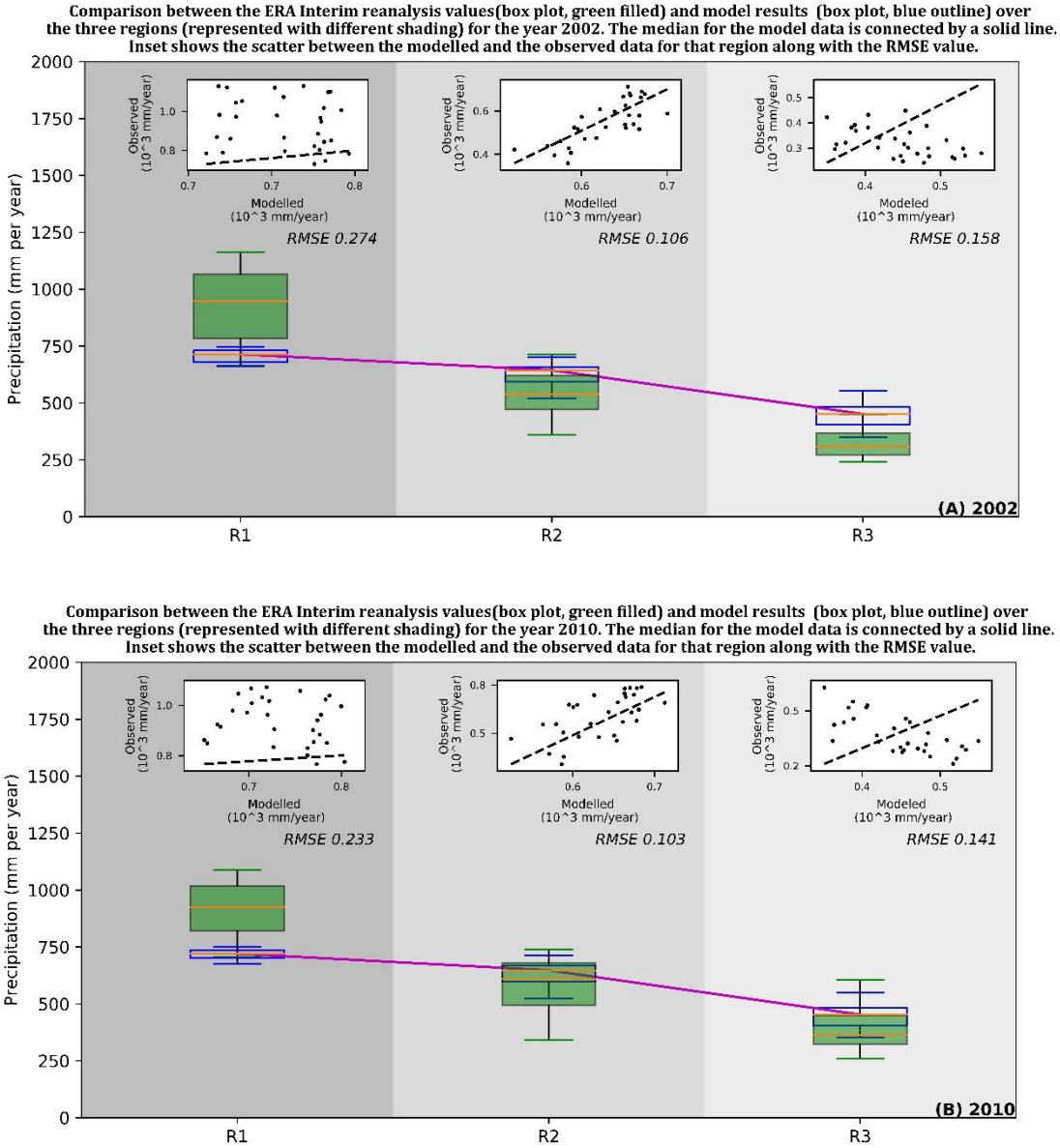

Figure 15 Comparison between the ERA-Interim reanalysis values and the model results over the three regions for ***Precipitation****. The solid line connects the median of the modeled data. Also shown in the inset are the scatter plots of the observed vs modeled data along with the RMSE (10^3 mm/year) values.*

The box plots in Figure 15 compares the modeled (blue outline) precipitation with the reanalysis data (green filled) for both analysis period in the three regions. The three regions are marked in succession with different shading and in the order of moisture movement. Figure 15A plots the modelled and the observed precipitation for the years 2002 (second modeled year) and Figure 15B plots the same for 2010 (last of the 10-year data). The inset plot shows the scatter of the observed vs modeled data with a 1:1 line drawn across it. The root mean square error (RMSE) for all the regions and both the years is calculated and represented in 10^3 mm per year. RMSE has the same units as the data being estimated. The RMSE values, as well as the box plots for the R1,

indicating that this model does not mirror the observed data that accurately. However, for the R2 and R3, the model works better for both the analysis years (i.e. 2002 and 2010).

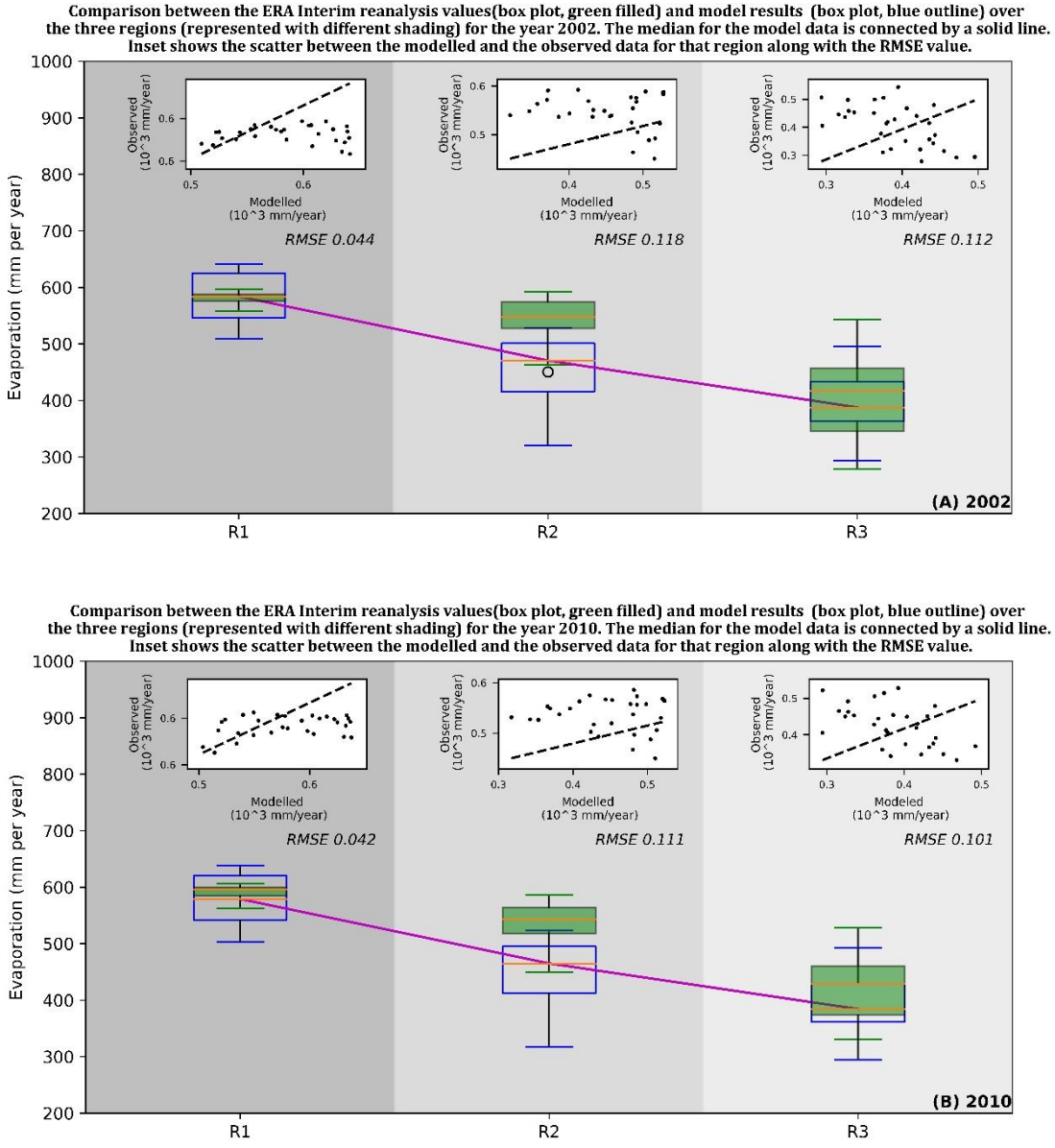

Figure 16 Comparison between the ERA-Interim reanalysis values and the model results over the three regions for ***Evaporation****. The solid line connects the median of the modeled data. Also shown in the inset are the scatter plots of the observed vs modeled data along with the RMSE (10^3 mm/year) value.*

Similarly, Figure 16 depicts the modelled and the observed evaporation for the two analysis years and the three regions. The box plots represent the modeled (blue outline box plot) and the observed (green filled box plot). The 1:1 line and the scatter plots are similar to the precipitation plots. However, the RMSE (mm per year) values are much better for the two years and for all the three regions.

4.3 Land Cover Change

This section addresses the first research question. The land cover changes from 2002 to 2011 and then to 2031, is shown below in Figure 17. Major changes can be seen at two locations; at the northern part near Colombia and Venezuela and the southern Brazil and Bolivia.

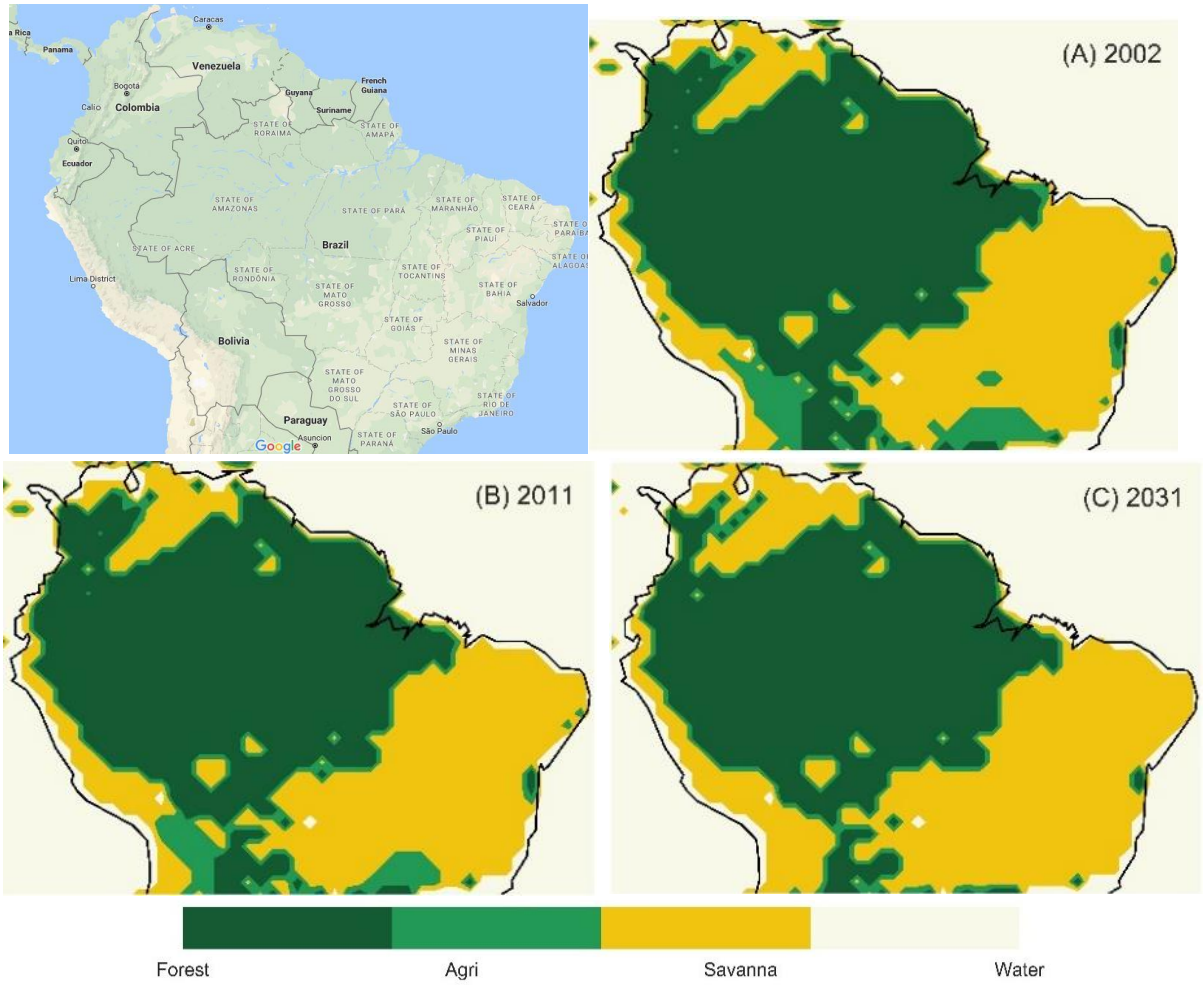

Figure 17 Google Maps image snipped on 19.09.17 and modelled land cover change from (A) 2002 to (B) 2011 to (C) 2031

Maximum change is observed in the *Rondonia* state of Brazil, *Mato Grosso* state of Brazil, the southern part of Colombia, and Bolivia. The change is expected in these areas because of their proximities to the existing dwellings and lower forest fractions. Also, in the states of Minas Gerais and Sao Paulo, complete removal of agriculture is observed. The west region of Bolivia, which used to have agriculture is also predicted to convert completely into savannas. The three sub-figures in Figure 17 look quite similar to each other, therefore, to depict the changes better, the fractional change in agricultural and forested areas are also presented in Figures 18-20. Three sets of plots are shown here; the absolute change in fraction of agriculture, absolute change in fraction of forest, and the percentage change in fractions of agriculture between 2002 and 2011, and between 2002 and 2031.

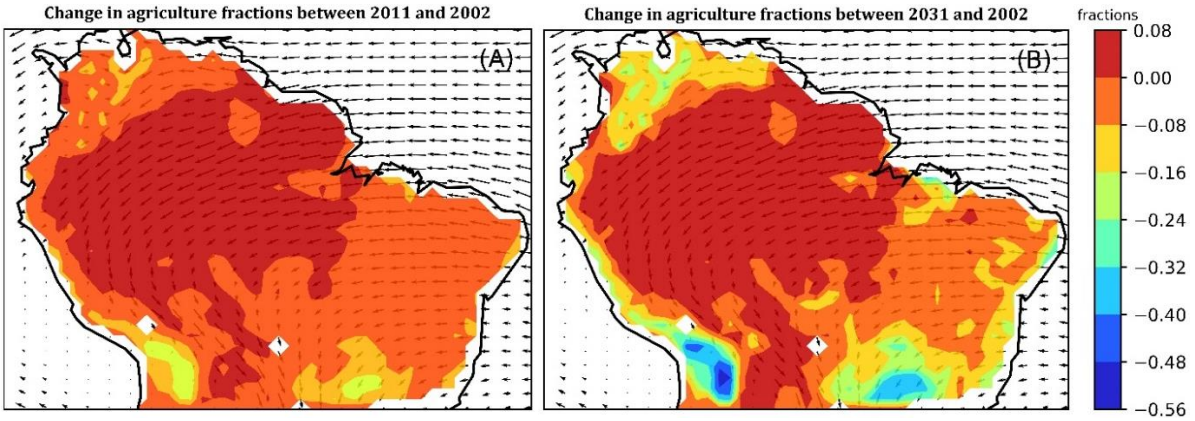

Figure 18 Change in agricultural fractions with January wind pattern in the background. (A) Fraction in 2011 - fraction in 2002, (B) Fraction in 2031 - fraction in 2002

Figure 18(A) shows the change in the agricultural fractions over the years. They have been calculated by subtracting the agricultural fractions of the year 2011 from the agricultural fractions of the year 2002. For example, a value of -0.4 would depict a decrease in agriculture fraction by 0.4 in that pixel. Similarly, figure 18(B) represents the change in agricultural fractions from 2002 to 2031. The positive values indicate an increase in the fractions, whereas the negative values indicate the decrease in the fractions.

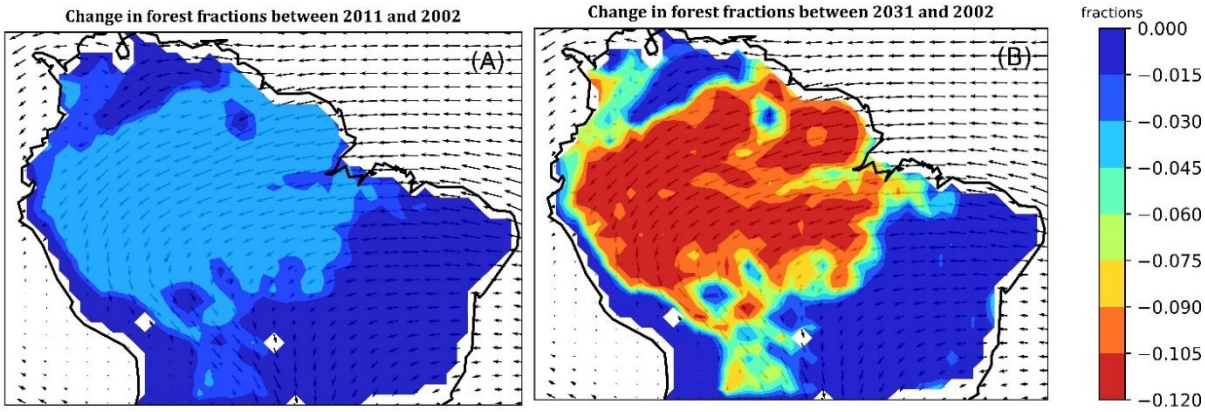

Figure 19 Change in forest fractions with January wind patterns in the background. (A) Fraction in 2011 – fraction in 2002, (B) Fraction in 2031 – fraction in 2002

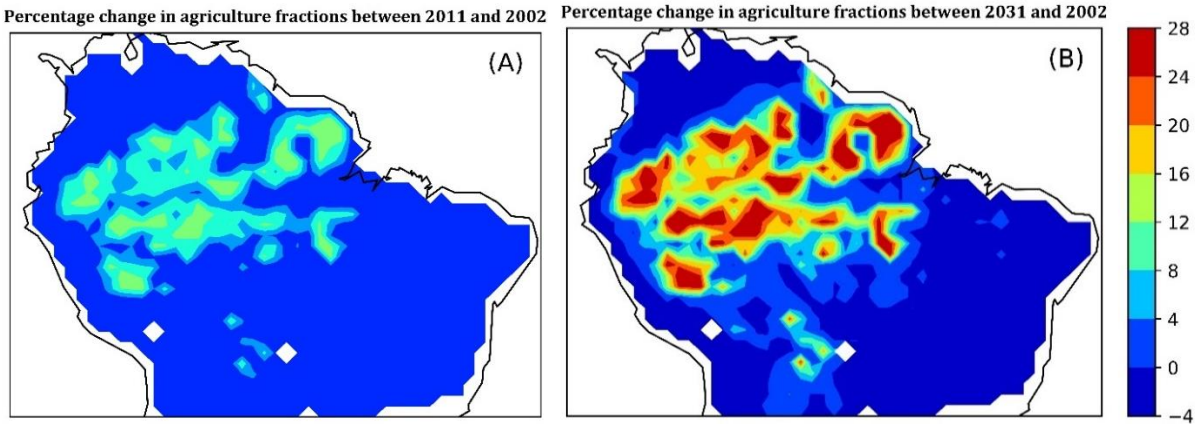

Figure 20 Percentage change in agriculture fractions with 2002 as the base year. (A) From 2002 to 2011, ((B) From 2002 to 2031

Figure 19 shows the change in the forest fractions, which follows the same pattern as the figure 18, with only negative values, as the forest fractions and the area are always reducing. Figure 20 shows the percentage change in the fractions, i.e. fraction change divided by fraction in 2002 * 100. The majority increase is observed in the Amazon rainforest, due to the fact that it had the least area of agriculture fractions to start with.

The forcing of the conversion from forest to agriculture is based on the soybean prices, and hence, the forest fractions can either remain constant or get converted to agriculture. On the other hand, the change in agriculture fractions, i.e. abandonment, is forced by maximum precipitation in the previous year. The agriculture fraction change is affected by both the conversion from forest to agriculture and the conversion from agriculture to savanna. On an average, a pixel loses 5 percent of its forest to make way for agriculture. This conversion is spatially spread because the global soybean price forcing is applied everywhere. In reality, there are remote regions in the Amazon rainforest, where agriculture is impossible as it is physically unapproachable. There are government mandated schemes in Brazil to conserve and preserve the rainforest Macedo *et al.*, (2012).

Maximum change is observed in the central region of the study area because it has the maximum forest fraction to start with. The maximum forest and agriculture fractions for the three regions and the entire study area and for the three analysis years (i.e., 2002, 2011, 2013) are mentioned in Table 11. The fractions in R3 are heavily reducing due to land cover types in that region as well as the reduction of forest cover in the upstream region. The land cover change model, takes only the soybean as the only exogenous (or external) forcing to calculate the land cover. Maximum annual rainfall is internal to the regional water balance dynamics, hence endogenous. To generate maps for the thirty-year simulation, the 2001 to 2010 global soybean prices are cycled to go on for additional twenty years. This may have a dampening effect on the land cover change. For a scenario in which the soybean prices are assumed to increase at currently observed rate, the land cover change is even more severe.

The land cover map of 2031 (figure 17(C)) also shows complete removal of forest from the North-west part of the study area. The forcing everywhere is the same, but the main reason for this wipe out is the wind intensities in the area. By analysing the wind patterns over the year, it is concluded that as the wind patterns diverge away before they enter that region. This implies that the moisture transport to that region is limited and hence, the complete removal of forests and in time even the agriculture. The pattern of change over the thirty years seems similar in space, however, the intensities are higher. In the agriculture fractions (figure 20(B)) the percentage increase in some regions is as high as 28 percent.

Table 10 Maximum forest and agriculture fractions for the three analysis years for the study area and the three sub regions

	Maximum Forest Fraction 2002	Maximum Forest Fraction 2011	Maximum Forest Fraction 2031	Maximum Agriculture Fraction 2002	Maximum Agriculture Fraction 2011	Maximum Agriculture Fraction 2031
R1	0.997	0.960	0.886	0.123	0.120	0.117
R2	0.995	0.959	0.884	0.277	0.236	0.168
R3	0.810	0.777	0.716	0.319	0.266	0.182
Study Area	0.997	0.961	0.886	0.944	0.750	0.750

In space, the hotspots are the same, but their intensities are much higher for both 2011 and 2031 runs. These regions, especially R2 which is at the cusp of two different land cover regions, are the most susceptible to this change. First, they have the Amazon rainforest on it's upwind, which is

pumping and regulating the precipitation in its downwind areas. Any damage to that would have adverse effects on R2, which is visible in our model output. Second, due to the region's proximities with the residential and existing farmlands, it would be the most susceptible to deforestation and change. Even with the condition that the previously cleared lands are used to cultivate the soybean and or other crops, eventually, these areas would be the first one to be cleared.

4.4 Change in Water Balance

This section addresses the second research question. The forest fractions change along with the agriculture fraction change and the corresponding change in the precipitation and evaporation data for the three regions and between the years is analyzed. To depict the land cover interaction, the model is run for a constant land cover type for both the analysis periods, i.e., 10 and 30 years starting from 2001. The constant land cover precipitation values for the three regions are subtracted from the modeled 'coupled' land cover precipitation values, i.e. when landcover changes in response to maximum precipitation and soybean prices. The same procedure is carried out for the evaporation data. The analysis is carried out for 2002, 2010 and 2030; 2002 is the first modeled year data and 2010 and 2030 being the last years in the two analysis periods. Six sets of differences are created; for every region and for the analysis years. Figure 21(A) shows the change in modeled forest fractions from 2002 to 2011 for the three regions. Figure 21(B) shows the modeled reduction in precipitation in 10 years due to the constraints forced by the model, and similarly, figure 21(C) shows the reduction in evaporation in 10 years. Figure 22 shows similar results as figure 21 but for 30 years simulations. The effect of current year's modelled precipitation is observed in the next years land cover. Therefore, the effect of 2010 and 2030's precipitation and evaporation are depicted in the land cover data of 2011 and 2031.

The maximum reduction in precipitation in 10 years and 30 years for the three regions is about 14 mm per year and 25 mm per year, respectively. These may not be big numbers, but it shows that the reduction in precipitation of a region is correlated with a decrease in the forest fraction. This is also dependent upon the reduced moisture flux from the upwind regions. Change in upwind conditions have a considerable impact on the downwind precipitation and in turn the evaporation. With a decrease of 3.6 percent in the forest fraction (for a pixel of 12, 100 km^2), the reduction in the precipitation and evaporation is 14 and 12 mm per year, respectively. As the forest fraction reduces, the evaporation in that region or pixel decreases too and eventually, the precipitation in the downstream region/pixel should decrease. A maximum change in evaporation of region 1 in figure 21(C) of 8 mm per year causes a maximum decrease in precipitation of region 2 in figure 21(B) by 9 mm per year. And subsequently, a maximum change in evaporation of region 2 in figure 21(C) of 11 mm per year causes a maximum decrease in precipitation of region 3 in figure 21(B) by 13 mm per year.

The decrease in the forest fraction of region 1 and region2 is similar, but the decrease in evaporation is higher in the region 2. This is attributable to the land cover distribution in the region and the precipitation trend in the past. Region 1 has forest as the dominant land cover type, whereas, the region 2 is mixed, and hence less forest cover overall. Figure 22(A) depicts the change in fraction over thirty years. The median change in fraction in region 1 and 2 both is around 11 percent per pixel of 12100 km^2 area. A maximum decrease of evaporation (figure 22(C)) of 23 mm per year in region 1 causes a maximum decrease of precipitation (figure 22(B)) by 26 mm per year in the region 2. Also, if the precipitation in the past is decreasing, then it will lead to higher soil moisture deficit, which in turn is going to further reduce the evaporation.

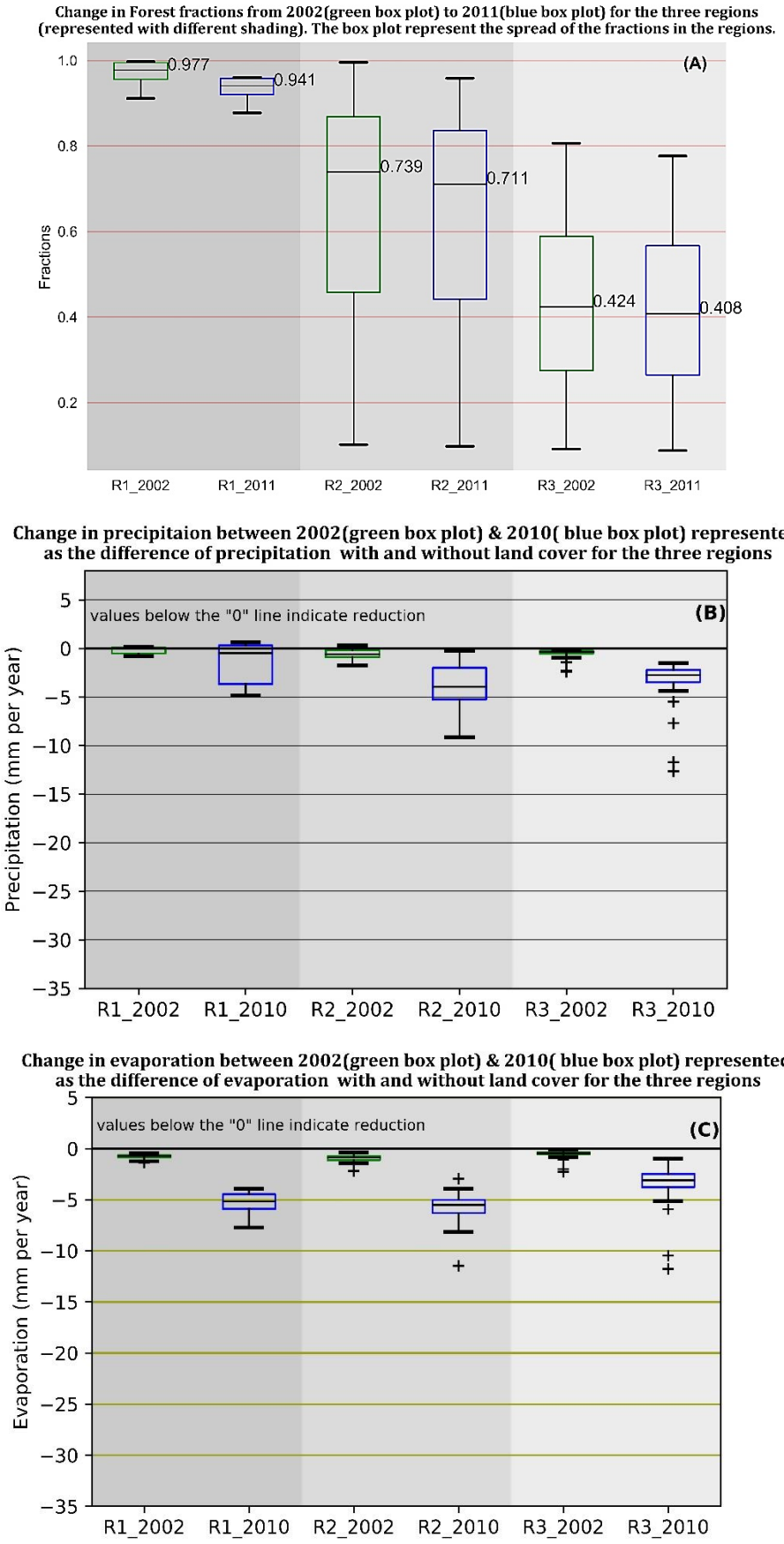

*Figure 21 (**A**) represent the forest fraction change in the three regions from 2002 to 2011, **(B)** represent the difference between the constant and changing land cover precipitation data from 2002 to 2010, **(C)** represent the difference between the constant and changing land cover evaporation data from 2002 to 2010.*

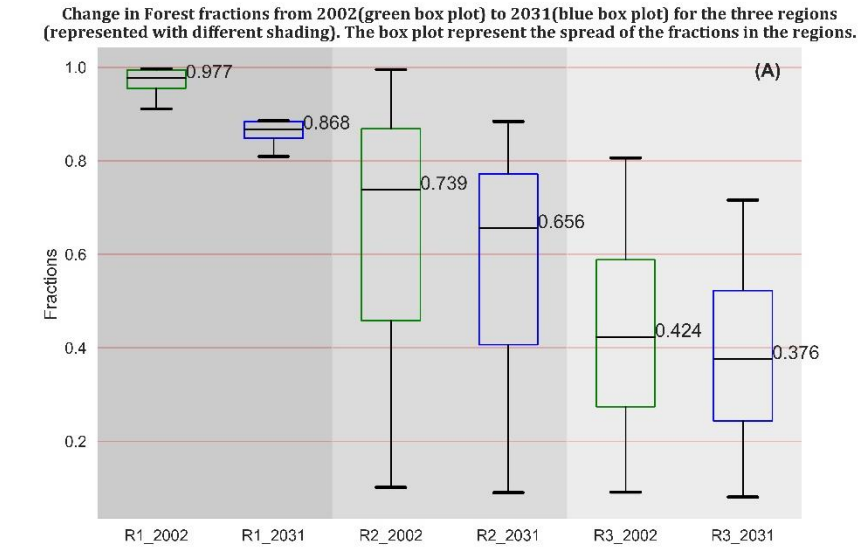

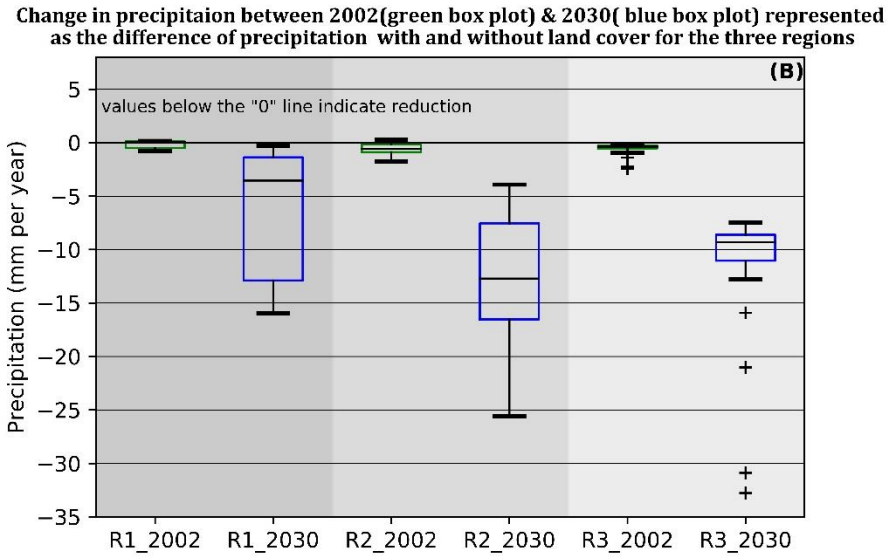

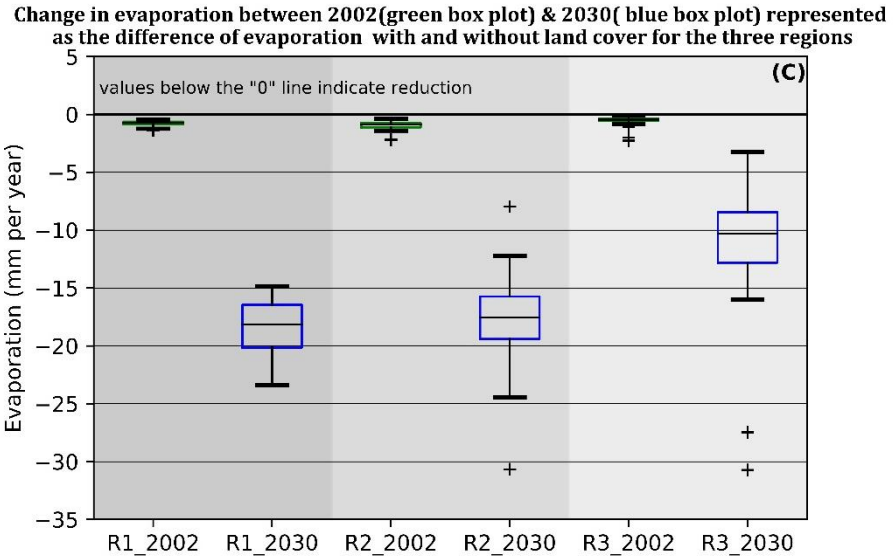

Figure 22 ***(A)*** *represent the forest fraction change in the three regions from 2002 to 2031,* ***(B)*** *represent the difference between the constant and changing land cover precipitation data from 2002 to 2030,* ***(C)*** *represent the difference between the constant and changing land cover evaporation data from 2002 to 2030.*

And similarly, a maximum decrease of evaporation (figure22(C)) of 31 mm per year may cause a maximum decrease of precipitation (figure 22(B)) by 33 m per year in region 3. The change in precipitation is less than expected because it is linearly related to the atmospheric moisture storage. On the other hand, evaporation is dependent upon the subsurface water available and the precipitation, therefore, the reduction is more prominent. In case of a reduction in subsurface available, the evaporation is directly affected, if the soil is not replenished with groundwater, which is a relatively slower process than the atmospheric moisture movement.

The maximum reduction of 26 mm per year in precipitation in a region (region 2) of median precipitation of 700 mm per year (i.e., 4%) is quite substantial. Similarly, region 3 has a maximum precipitation reduction of precipitation of 33 mm per year, with only 500 mm per year (i.e., 7%) median precipitation value. [Spracklen, Arnold and Taylor, (2012)] observed a 20 percent reduction in wet season precipitation over 50 years. These calculations were carried out on the business as usual scenarios for both dry and wet seasons. The maximum 20 percent reduction is observed in region R3 in this research. In case of the dry season, the maximum reduction went up as high 40 percent in region R3. In this research, the annual precipitation reduction is considered along with the soybean fuelled land cover change, and hence the difference in percentages. Zemp *et al.*, (2017) found a reduction of mean annual precipitation by 32 mm per year in the Amazon basin by using 12-year (2000 – 2012) rainfall data from TRMM 3B42. Lejeune *et al.*, (2015) carried out a similar study with three scenarios, 50 percent deforestation, intermediate, and total deforestation in the Amazonian region. They used the ERA-Interim data from 1987 to 2010 for their simulations and predicted a reduction in mean annual precipitation of 2.7, 4.1, and 5.3% for respective scenarios, which is moderately close to this research's output. However, the fractional change in the areas at the cusp of savannas and rainforest are assumed to be correct as Zemp *et al.*, (2017) has demonstrated a reduction of 14 percent in the Amazon rainforest under reduced moisture flow – similar to the conclusion of our study.

The model created is run for only the ERA-Interim data and therefore brings along any bias the source data has. Since the wind intensities have not been modeled, the results are completely based on the reduction of the atmospheric moisture due to the change in land cover. However, these changes and interactions are not local. Landcover changes upwind of R1 influences both precipitation and evaporation in the selected regions, in addition to local more immediate effects of land cover changes. Ideally, reduced forest cover, changing albedo, and increasing surface temperatures can cause a reduction in the wind intensities. Also, the localized interpolation scheme used to stabilize the atmospheric moisture's divergence may have smoothened out the amplitude variation. This can cause under prediction in areas with convergence. The land cover change due to soybean prices is forced all over the study area, and hence the fractional change in the central Amazon is being overpredicted.

5. Conclusions and Recommendations

In this research, a distributed model for northern South America is created to understand the interlinkages between soybean prices, deforestation and regional water balance. The model estimates the changes in atmospheric moisture fluxes due to changes in the land cover, as forced by the agriculture expansion in the region. This research is carried out to quantify this change and understand the behaviour. This research is also aimed at understanding the adverse effects of clearing out the rainforests. It explains the notion that deforestation at one location has a much larger spectrum of effects in the downwind areas in terms of both precipitation and evaporation, which in turn may induce further landcover changes downwind (e.g. abandonment of agricultural areas and its conversion to savannas).

This works adds on to the previous studies carried out mentioned in chapter 1 which has shown the importance of the Amazon rainforest. This research has shown that the modeled land cover does not completely reduce to savannas, which is in agreement with previous studies, however, in case of an extreme reduction in precipitation due to climate change and/or prolonged droughts, the rainforests may lead to complete dieback. With the soybean price as forcing in the model, it is concluded that,

1. A reduction of 3.6 percent per 12000 square kilometers in the forest areas expected in the majority of areas, in ten years. This seemingly insignificant percent reduction causes a more significant reduction in precipitation in downwind areas.
2. A reduction of 14 and 35 mm per year in precipitation in ten and thirty years, respectively due to the reduction of forest fractions in upwind regions was estimated
3. A reduction of 12 and 33 mm per year in evaporation in ten and thirty years in the downwind region (R3), respectively due to the reduction of forest fractions in the upwind region (R2).
4. Regions on the cusp of rainforest and residential dwellings are the most susceptible to complete conversion, like R2 region in this research shown in figure 15 and figure 17.
5. An increase in the percentage agriculture area per pixel of around 10 and 28 percent per pixel in the next ten years and thirty years, respectively. This increase in area is dependent upon the soybean prices.
6. Regions with varying wind directions over the seasons have a higher probability of being affected by the land cover change, like the north-western areas of the study area.

The presence of biotic pumping of rainforest is concluded by the reduction in precipitation in downwind regions due to changes in land cover in upwind regions. The reduction in the precipitation and evaporation values are due to the changing land cover and not due to natural reduction is proved by taking the difference of the modeled values with the constant land cover values. Due to our conservative approach towards the forcing factors of deforestation, several additional possible feedbacks in the coupled system have been neglected. For example, any interaction from the land protection lobby is not taken in to account. It is also curious to understand the importance of these protection schemes, because, based on this research's results, in the absence of these regulations, the whole region is vulnerable to deforestation. Since the government of Brazil has enforced strict regulations against the deforesters, the farmers have been forced to cultivate on the previously cleared lands. This has reduced the deforestation rate considerably. But this "previously cleared land" would only be used for one or two years, after which newer areas would be needed. Similarly, there is some counter stabilizing factors which may push the possible tipping points to a safer point, but we have not included them in this research.

The research tries to explain the food-water nexus and why it is of such importance for the region. The study region is abundant in the food and water resources, and these resources have been harnessed by the countries lying in the region to fuel economic growth. As it follows from the result of second research question, if the Latin America and the Caribbean are to sustain their food producing capabilities for the future, the conservation practices, like the ones in Brazil have to be followed strictly. Brazil may not be the ideal role model due to the recent instances of trying to relax the legislation, however, it is the only country with such sanctions. Also, it contains the maximum percentage of Amazon rainforest and hence, should drive the proactive conservation. The result of the first research question dictates that the average reduction in precipitation in the region is directly proportional to the reduction in the percentage fraction of forests. The change in precipitation shed of the region is going to affect the agricultural practices in the region.

UNESCO's biosphere reserves around the world have contributed to the understanding of the complex systems. The biosphere reserve in the central Amazon needs to create outreach programmes for the agricultural community. The global soybean prices are out of the local government's control, but new agricultural practices will have to utilize in the area to speed up the nutrition levels of the soil already used for soybean. The government has provided subsidies to the farmers who have been cropping in the previously cleared land and those farmers are isolated who fail to comply with the rules. Other countries need to emulate Brazil in endorsing the conservation approach. The countries need to look at the bigger picture. While progressing towards financial gains, it is vital to realize the effect of rampant encroachment to the ecological balance.

Based on current model formulations and its limitations, following recommendations are made,

1. The time step of the water balance calculations can be reduced to increase the stability of the model. Instead of monthly time steps, if the model is reduced to a daily, or 6 hourly time steps, the stability due to the wind speed time step can be increased further.
2. Along with modelling the atmospheric moisture, the change in wind intensities may also be modelled. Due to reduced evaporation, and change in the atmospheric pressure, the wind intensities may change as well. This could further reduce the atmospheric moisture transport in the downwind regions.
3. Instead of using ERA-Interim data over the Amazon, other rainfall datasets, like TRMM, Climate Research Unit (CRU), the Global Precipitation Climatology Centre (GPCC), the Global Precipitation Climatology Project (GPCP), etc.
4. In order to further investigate the biotic pumping effect, three regions, close to the east coast of the study area may be selected. With the first region over the ocean, the second over the continent, and the third region inside the continent in continuation with the wind movement. And the change in precipitation in the third region can be recorded as an effect of a change in land cover change over the second region.
5. A more comprehensive modelling approach, by considering all of the above, will definitely provide better and more stable results.

6. References

Achard, F. *et al.* ((2002) 'Determination of deforestation rates of the world ' s humid tropical forests', *Science*, 297(August), pp. 999–1002. doi: 10.1126/science.1070656.

Bagley, J. E. *et al.* ((2012) 'Effects of land cover change on moisture availability and potential crop yield in the world's breadbaskets', *Environmental Research Letters*, 7(1), p. 14009. doi: 10.1088/1748-9326/7/1/014009.

Bellfield, H. and Sabogal, D. ((2016) *Applying The Water-Energy-Food Nexus In The Amazon*, *Ecosystem Marketplace*. Available at: http://www.ecosystemmarketplace.com/articles/applying-water-energy-food-nexus-amazon/ (Accessed: 23 October 2017).

Berrisford, P. *et al.* ((2009) 'The ERA-Interim Archive', *ERA report series*, 1(1), pp. 1–16. Available at: http://www.ecmwf.int/publications/library/do/references/list/782009.

Betts, A. K., Köhler, M. and Zhang, Y. ((2009) 'Comparison of river basin hydrometeorology in ERA-Interim and ERA-40 reanalyses with observations', *Journal of Geophysical Research Atmospheres*, 114(2). doi: 10.1029/2008JD010761.

Boers, N. *et al.* ((2017) 'A deforestation-induced tipping point for the South American monsoon system', *Scientific Reports*. Nature Publishing Group, 7(January), p. 41489. doi: 10.1038/srep41489.

Budyko, M. I. ((1972) 'The future climate', *Eos, Transactions American Geophysical Union*, 53(10), p. 868. doi: 10.1029/EO053i010p00868.

Bunyard, P. *et al.* ((2014) 'Analysis of Meteorological Data for La Selva Station by Applying the Biotic Pump Theory', 9(16), pp. 73–77.

Chaherli, N. and Nash, J. ((2013) *Agricultural Exports from Latin America and the Caribbean: Harnessing Trade to Feed the World and Promote Development*.

Coe, M. T. *et al.* ((2013) 'Deforestation and climate feedbacks threaten the ecological integrity of south-southeastern Amazonia.', *Philosophical transactions of the Royal Society of London. Series B, Biological sciences*, 368(1619), p. 20120155. doi: 10.1098/rstb.2012.0155.

Davidson, E. a. *et al.* ((2012) 'The Amazon basin in transition', *Nature*, 481(7381), pp. 321–328. doi: 10.1038/nature10717.

Dee, D. P. *et al.* ((2011) 'The ERA-Interim reanalysis: Configuration and performance of the data assimilation system', *Quarterly Journal of the Royal Meteorological Society*, 137(656), pp. 553–597. doi: 10.1002/qj.828.

Dobrovolski, R. and Rattis, L. ((2015) 'Water collapse in Brazil: The danger of relying on what you neglect', *Natureza e Conservacao*. Associação Brasileira de Ciência Ecológica e Conservação, 13(1), pp. 80–83. doi: 10.1016/j.ncon.2015.03.006.

Dorst, J. P. and Knapp, G. W. ((2017) *South America*, *Encyclopædia Britannica, inc.*

Eltahir, E. A. B. and Bras, R. L. ((1994) 'Precipitation recycling in the Amazon basin', *Quarterly Journal of the Royal Meteorological Society*, 120(518), pp. 861–880. doi: 10.1002/qj.49712051806.

Van Der Ent, R. J. *et al.* ((2010) 'Origin and fate of atmospheric moisture over continents', *Water Resources Research*, 46(9), pp. 1–12. doi: 10.1029/2010WR009127.

Flachsbarth, I. *et al.* ((2015) 'The role of Latin America's land and water resources for global food security: Environmental trade-offs of future food production pathways', *PLoS ONE*, 10(1), pp. 1–24. doi: 10.1371/journal.pone.0116733.

Foley, J. a *et al.* ((2005) 'Global consequences of land use.', *Science (New York, N.Y.)*, 309(5734), pp. 570–4. doi: 10.1126/science.1111772.

Gordon, L. J. *et al.* ((2005) 'Human modification of global water vapor flows from the land surface', *Proceedings of the National Academy of Sciences*, 102(21), pp. 7612–7617. doi: 10.1073/pnas.0500208102.

INPE (no date) *National Institute for Space Research*. Available at: http://www.inpe.br/ingles/ (Accessed: 24 October 2017).

Kavetski, D. and Clark, M. P. ((2010) 'Ancient numerical daemons of conceptual hydrological modeling: 2. Impact of time stepping schemes on model analysis and prediction', *Water Resources Research*, 46(10), pp. 1–27. doi: 10.1029/2009WR008896.

Laurance, W. F. ((2004) 'Pervasive alteration of tree communities in undisturbed Amazonian forests', *letters to nature*, 428, pp. 171–175. doi: 10.1038/nature02383.

Leck, H. *et al.* ((2015) 'Tracing the Water-Energy-Food Nexus: Description, Theory and Practice', *Geography Compass*, 9(8), pp. 445–460. doi: 10.1111/gec3.12222.

Lejeune, Q. *et al.* ((2015) 'Influence of Amazonian deforestation on the future evolution of regional surface fluxes, circulation, surface temperature and precipitation', *Climate Dynamics*, 44(9–10), pp. 2769–2786. doi: 10.1007/s00382-014-2203-8.

Lettau, H., Lettau, K. and Molion, L. C. B. ((1979) 'Amazonia's Hydrologic Cycle and the Role of Atmospheric Recycling in Assessing Deforestation Effects', *Monthly Weather Review*, pp. 227–238. doi: 10.1175/1520-0493(1979)107<0227:AHCATR>2.0.CO;2.

Macedo, M. N. *et al.* ((2012) 'Decoupling of deforestation and soy production in the southern Amazon during the late 2000s', *Proceedings of the National Academy of Sciences*, 109(4), pp. 1341–1346. doi: 10.1073/pnas.1111374109.

Makarieva, A. and Gorshkov, V. G. ((2006) 'Biotic pump of atmospheric moisture as driver of the hydrological cycle on land', *Nuclear Physics*, pp. 2621–2673. doi: 10.5194/hessd-3-2621-200.

Makarieva, A., Gorshkov, V. and Li, B. ((2013) 'Revisiting forest impact on atmospheric water vapor transport and precipitation', *Theoretical and applied climatology*, (2013), pp. 1–29. doi: 10.1007/s00704-012-0643-9.Electronic.

Malhi, Y. *et al.* ((2009) 'Exploring the likelihood and mechanism of a climate-change-induced dieback of the Amazon rainforest', *Proceedings of the National Academy of Sciences*, 106(49), pp. 20610–20615. doi: 10.1073/pnas.0804619106.

Moore, N. *et al.* ((2007) 'Uncertainty and the changing hydroclimatology of the Amazon', *Geophysical Research Letters*, 34(14), pp. 1–5. doi: 10.1029/2007GL030157.

ORNL DAAC ((2017) *Spatial Data Access Tool (SDAT)*, *ORNL DAAC; Oak Ridge; Tennessee; USA.* Available at: https://doi.org/10.3334/ORNLDAAC/1388 (Accessed: 8 February 2017).

Oyama, M. D. and Nobre, C. A. ((2003) 'A new climate-vegetation equilibrium state for tropical South America', *Geophysical Research Letters*, 30(23), p. 2199. doi: 10.1029/2003GL018600.

Satyamurty, P., da Costa, C. P. W. and Manzi, A. O. ((2013) 'Moisture source for the Amazon Basin: A study of contrasting years', *Theoretical and Applied Climatology*, 111(1–2), pp. 195–209. doi: 10.1007/s00704-012-0637-7.

Savenije, H. H. G. ((1996) 'Does Moisture Feedback Affect Rainfall Significantly?', *Elsevier Science Ltd*, 20(5), pp. 507–513. doi: 0079-1946/95.

Scott, C. E. ((2016) *The Biogeochemical Impacts of Forests and the Implications for Climate Change Mitigation*. Springer.

da Silva, R. R., Werth, D. and Avissar, R. ((2008) 'Regional impacts of future land-cover changes on the Amazon basin wet-season climate', *Journal of Climate*, 21(6), pp. 1153–1170. doi: 10.1175/2007JCLI1304.1.

Spracklen, D. V., Arnold, S. R. and Taylor, C. M. ((2012) 'Observations of increased tropical rainfall preceded by air passage over forests', *Nature*. Nature Publishing Group, 489(7415), pp. 282–285. doi: 10.1038/nature11390.

Turzi, M. ((2012) 'The political economy of South America ' s soybean chain Mariano Turzi'.

UN-Water ((2006) 'Water: A Shared Responsibility The United Nations World Water Development Report', *Water Resources*, (3), pp. 120–156. doi: 10.7748/nm.21.4.12.s12.

UNDP ((2015) 'Sustinable Develpment Goals'.

World Bank ((2013) 'World Bank Annual Report', *Annual Report 2013*, p. 63. doi: 10.1596/978-0-8213-9937-8.

WWF ((2016) *Living Amazon Report 2016: A regional approach to conservation in the Amazon*.

Zemp, D. C. *et al.* ((2017) 'Self-amplified Amazon forest loss due to vegetation-atmosphere feedbacks', *Nature Communications*. Nature Publishing Group, 8, p. 14681. doi: 10.1038/ncomms14681.